Cognitive Hybrid Division Duplex for Two-Tier Femtocell Networks

Yong Sheng Soh, *Member, IEEE*, Tony Q. S. Quek, *Senior Member, IEEE*,
Marios Kountouris, *Member, IEEE*, and Giuseppe Caire, *Fellow, IEEE*,

***Abstract*—With the exponential increase in high rate traffic driven by a new generation of wireless devices, data is expected to overwhelm cellular network capacity in the near future. Femtocell networks have been recently proposed as an efficient and cost-effective approach to provide unprecedented levels of network capacity and coverage. However, the dense and random deployment of femtocells and their uncoordinated operation raise important questions concerning interference pollution and spectrum allocation. Motivated by the flexible subchannel allocation capabilities of cognitive radio, we propose a cognitive hybrid division duplex (CHDD) which is suitable for heterogeneous networks in future mobile communication systems. Specifically, this CHDD scheme has a pair of frequency bands to perform frequency division duplex (FDD) on the macrocell while time division duplex (TDD) is simultaneously operated in these bands by the underlaid cognitive femtocells. By doing so, the proposed CHDD scheme exploits the advantages of both the FDD and TDD scheme: operating FDD at the network level manages inter-tier interference while operating TDD at the femtocell level provides femtocells the flexibility of adjusting uplink and downlink rates. Using tools from stochastic geometry and capturing the spatial randomness, we provide a methodology on how to design the optimal switching mechanism for cognitive TDD operation of femtocells. Specifically, we derive performance measures in terms of success probability, total network throughput, and spatial average capacity for the proposed CHDD scheme for macro tier in downlink and uplink mode, respectively. We propose an open access policy on our CHDD scheme to improve the performance of macrocell transmissions. Our analysis and numerical results show the effectiveness of introducing cognition in femtocells so as to improve the system performance of the overall two-tier femtocell networks.**

***Index Terms*—Femtocell network, cognitive radio, frequency division duplex, time division duplex, stochastic geometry**

I. Introduction

Mobile cellular networks have been undebatably a success story, which resulted in wide proliferation and demand for ubiquitous heterogeneous broadband mobile wireless services. Cellular operators are integrating *small cells* as a means to provide dedicated additional capacity either where most data usage generally occurs (i.e. enterprises, households) or where users are likely to experience poor throughput performance (i.e. cell edges, subway stations, and households). Small cells such as femtocells offer radio coverage through a given wireless technology while a broadband wired link connects them to the backhaul network of a cellular operator [1]–[3]. Such technical solution presents several benefits both to operators and end consumers. The latter obtains enhanced coverage, better support for high data rate services, and a prolonged battery life for their devices. The advantages mainly come from the reduced distance between the end-user terminal and the access point as well as from the limited number of users served by a small cell access point.

One of the major challenges in femtocell development is the incursion of inter-tier interference due to aggressive frequency reuse. This can deteriorate the effectiveness of the femtocell architecture [4]–[6]. Hence, interference modeling is an important topic and stochastic geometry has recently gathered considerable attention as a powerful, accurate, and flexible tool to model interference [7]–[10]. Modeling macrocell base stations (MBSs) with a homogeneous Poisson point process (PPP) and associating macrocell users to the closest MBS is an extensively used approach. While there is a concern that in real-world networks the deployment of MBSs are well-planned and thus regular, recent work has shown that a PPP model approximates very closely to the traditional lattice or hexagonal model [11]. Femtocell access points (FAPs) are also extensively modeled as PPP, mainly because their deployment is usually uncoordinated. To introduce a positive correlation between the location of FAPs and the location of FAP users, one common approach is to distribute users conditioned on the location of the assigned FAP [12]–[14].

When both tiers share the whole spectrum, indoor user communication is hindered by interference from undesignated FAPs as well as MBSs, and the same holds for outdoor users. This problem is further exacerbated by the random deployment of FAPs, which are often installed and controlled by their subscribed users, thus making centralized interference management not viable. For spectrum allocation, a decentralized disjoint subchannel allocation scheme has been proposed to eliminate cross-tier interference [12]. While disjoint subchannel allocation is shown to be sensible in dense networks, it is not clear whether disjoint schemes are necessary in sparse networks, whereby the inter-tier interference incurred through spectrum sharing can be tolerated [14]. On the other hand, in [15], it was demonstrated by simulations that judiciously sharing a portion of subchannels between the two tiers is beneficial for maximizing throughput; however the spatial

Y. S. Soh and T. Q. S. Quek are with the Institute for Infocomm Research, A*STAR, 1 Fusionopolis Way, #21-01 Connexis South Tower, Singapore 138632. (e-mail: ysoh@i2r.a-star.edu.sg).

T. Q. S. Quek is with the Singapore University of Technology and Design, 20 Dover Road, Singapore 138632. (e-mail: qsquek@ieee.org).

M. Kountouris is with SUPELEC (Ecole Supérieure d'Electricité), Gif-sur-Yvette, France (e-mail: marios.kountouris@supelec.fr).

G. Caire is with the University of Southern California, Los Angeles, CA 90089, USA (e-mail: caire@usc.edu).

distribution of FAPs has not been fully captured. To further enhance throughput and manage interference, the concept of cognitive radio can be exploited by reusing underutilized portions of the licensed spectrum, provided that the transmissions of secondary radios do not cause harmful interference to primary users [16]–[19]. Applying the concept of cognitive radio to femtocell networks, we can view the macro and femto tiers as primary and secondary networks, respectively, except that the FAPs are deployed randomly and the number of FAPs can be significantly large [20]–[22].

Motivated by the flexible subchannel allocation capabilities of cognitive radio, we propose a cognitive hybrid division duplex (CHDD) that is suitable for heterogeneous networks in future mobile communication systems. This is different from previous related works in [23], [24] where only one of the frequency division duplex (FDD) frequency band is allowed to have time division duplex (TDD) operation by the femtocells. Our CHDD scheme allows TDD to simultaneously operate on both FDD bands by underlaying the cognitive femtocells in an intelligent manner. Specifically, cognitive radio enabled FAPs and femtocell users can sense the control channels of the macro tier to decide on how to operate in the TDD mode. Therefore, our CHDD two-tier network allows for simultaneous FDD and TDD operations by developing a statistical network mechanism to control interference as well as to optimize the uplink (UL) and downlink (DL) traffic. Based on the mathematically tractable two-tier network model in [14], we incorporate the concept of hybrid division duplex with underlaying cognitive femtocells. In addition, the UL and DL success probabilities, spatial average capacities, and total network throughput for each tier are derived in closed form for a given time slot, respectively.

When we consider a femtocell user in isolation, it is possible to allow the DL and UL demands to determine the proportion of time spent either DL or UL. The situation is less straightforward when we take into account the interference due to other mobile users in the vicinity. Specifically, since the devices used at the user and the FAP end are inherently different thereby leading to different transmit powers, one could ask the question if there are gains in strategies such as agreeing to transmit in DL (respectively UL) in the same time slots.

For the above reasons, we will we investigate the optimal uplink-downlink mode multiplexing probability of the underlying TDD cognitive femtocells that maximizes different system performance measures in a given time slot. Furthermore, we study the effect of open access FAP in our CHDD scheme and quantify the performance gain in terms of success probability. Numerical results show the effectiveness of our proposed CHDD scheme for improving the overall network performance and give a rule-of-thumb on how to choose the uplink-downlink mode multiplexing probability of the femto tier optimally. Overall, this work provides essential understanding for successful deployment of future cognitive femtocell networks.

The layout of this paper is as follows. In Section II, we present our system model and our CHDD scheme. In Section III, we present our performance analysis in terms of success probability, total network throughput, and spatial average capacity for our CHDD scheme. In Section IV, we present several optimization framework of CHDD scheme. In Section V, we provide some numerical results. Concluding remarks are given in Section VI.

II. System Model

A. Two-tier network model

The macrocell tier consists of MBSs and macrocell users, which are modeled as independent homogeneous PPPs $\Theta \sim \text{PPP}(\lambda_{\text{m}})$, $\tilde{\Theta} \sim \text{PPP}(\mu_{\text{m}})$ respectively [11]. MBSs and macrocell users transmit at constant powers P_{m} and Q_{m} respectively. Following [11], the MBS that is geographically closest to a macro user will be designated as the user's MBS. Since both Θ and $\tilde{\Theta}$ are stationary processes, the distribution of distance R_{m} between each MBS and its designated macro user pair will remain the same regardless of their exact locations, and its pdf is given by $f_{R_{\text{m}}}(r) = 2\pi\lambda_{\text{m}} r \exp(-\lambda_{\text{m}}\pi r^2)$ [11]. The femtocell tier consists of FAPs and femtocell users, where the set of FAPs is distributed according to a homogeneous PPP $\Phi \sim \text{PPP}(\lambda_{\text{f}})$. Each FAP is associated with a femtocell user at a constant distance R_{f} away at a uniformly random direction.[1] Thus, the set of femtocell users is distribute according to a point process $\tilde{\Phi}$ of intensity $\mu_{\text{f}} = \lambda_{\text{f}}$ (but not independent of Φ). The maximum transmit power of FAPs and femtocell users are denoted as P_{f} and Q_{f}, respectively. While we shall assume that $P_{\text{f}} > Q_{\text{f}}$ for simplicity, all results stated may be adapted to the case where $Q_{\text{f}} > P_{\text{f}}$. In the following, we will invoke Slivnyak's Theorem implicitly [7], such that when 'conditional on' a single point from a PPP being at the origin, the remaining points are distributed as a PPP as well. Furthermore, we assume that the geometry of the two-tier network is static as time varies and we denote the σ-algebra of the point processes $\sigma(\Theta, \tilde{\Theta}, \Phi, \tilde{\Phi})$ as $\mathcal{G}$.

B. Signal-to-interference ratio

For notational convenience, we denote a base station or a user by its location. For transmitter x and receiver u transmitting at time slot t, the signal-to-interference ratio (SIR) from x to u is

$$\mathsf{SIR}(x \to u) = \frac{P_x F_x^u(t) g(x-u)}{\sum_{y\in\Omega(x)} P_y F_y^u(t) g(y-u)} \tag{1}$$

where $\Omega(x)$ is the set of nodes in Ω that interferes with x, P_y is the power of the transmitting node at y, and $F_x^u(t)$ is the power fading coefficient from x to u at time t. In our model, we assume that $F_x^u(t) \sim \exp(1)$, i.e. the channel fading is Rayleigh distributed. We ignore background thermal noise since we consider an interference-limited regime such that interference is the dominating noise effect. The path loss function is denoted as $g(x) = \|x\|^{-\alpha}$, where α is the universal path loss exponent.

[1] It is true that FAP users are not all located at a uniform distance from the FAP, and thus R_{f} should be treated as a measure of the statistical average distance of FAP user from FAP. We will see that most results derived later on are independent of R_{f}, hence there is little benefit in assuming a statistical distribution of R_{f}. For exposition convenience, we shall assume that R_{f} is constant, however the effect of random distance can be easily incorporated in our analysis resulting though in involved expressions.

C. Performance metrics

Using (1), we can define the *success probability* from x to u as $\mathbb{P}(\mathsf{SIR}(x \to u) > \gamma)$, where γ is a prescribed threshold. Due to the stationarity of the point processes, the success probability for each pair of Tx-Rx in each tier is the same. Since we consider both uplink and downlink in our hybrid system, we denote $\gamma_{\mathrm{m}}, \gamma_{\mathrm{f}}, \eta_{\mathrm{m}}$, and η_{f} as the quality-of-service (QoS) thresholds for macro downlink, femto downlink, macro uplink, and femto uplink, respectively. Note that according to Slivnyak's Theorem, the statistics of the interference seen by any node in the network is the same if the nodes form a homogeneous PPP. This means that the distribution of the point process is unaffected by addition of a receiver at the origin and this receiver is called a typical receiver.

Next, we define the *throughput* in a single time slot as $\mathbb{P}(\mathsf{SIR} > \gamma)\log(1+\gamma)$, where $\mathbb{P}(\mathsf{SIR} > \gamma)$ is the success probability of the transmission and γ is a prescribed QoS threshold.[2] To have a measure of the amount of traffic within the network in a single instance, we define the *network throughput* as $\lambda\mathbb{P}(\mathsf{SIR} > \gamma)\log(1+\gamma)$, where λ is taken to be the density of the transmitters per unit area. This metric, also known as area spectral efficiency, essentially assumes that each MBS serves one user, at any one instance. As a result, the amount of network throughput is restricted to the density of transmitters, as opposed to the density of users. Finally, we define the *spatial average capacity* (in nats/Hz) achievable by a typical user assuming Shannon capacity achieving modulation and coding for the instantaneous SIR as $R = \mathbb{E}[\log(1+\mathsf{SIR})]$, where the SIR is also a random variable.

D. Cognitive hybrid division duplex

The main attractiveness of the CHDD is the capability of enabling both TDD operations and FDD operations in a heterogeneous system. Similar to conventional FDD mode, the macrocell operates with a pair of frequency bands for the UL and the DL. For simplicity, all macrocells are assumed to operate with frequency reuse one. Within each macrocell, our CHDD scheme allows the femtocells to operate on a TDD mode using both the FDD DL and UL spectrum. In this way, no additional spectrum is required for operating the underlaid femtocell network and they can employ cognitive radio technology to opportunistically utilize the FDD spectrum efficiently. The deployed frequency bands of the CHDD scheme are depicted in Fig. 1.

We assume that data is sent in time slots. In each time slot, each femtocell can be configured to be as *downlink* (d) or *uplink* (u) mode by accessing the available FDD bands. In d mode, FAPs transmit signals to the femtocell users; in u mode, the femtocell users transmit signals to the FAPs. Moreover, we assume that all the FAPs and femtocell users are able to sense the control channels of the macrocell tier in a cognitive manner [20]. In this way, FAPs and femtocell users can optimize the femtocell tier so as to maximize the system performance of the overall CHDD two-tier network. In the following, we will consider both the uplink and downlink FDD bands separately and investigate the performance of cognitive TDD femtocells in each FDD band separately. For macrocells, we assume that there is a centralized control in configuration by the network operators. In the downlink FDD band, all macrocells are simultaneously configured as downlink (D) in all the time slots. On the other hand, in the uplink FDD band, all macrocells are simultaneously configured as uplink (U) in all the time slots. For simplicity, we employ the same point processes Θ and $\tilde{\Theta}$ for both D and U modes. Figure 2 illustrates the two-tier CHDD system when macro tier is in D mode.

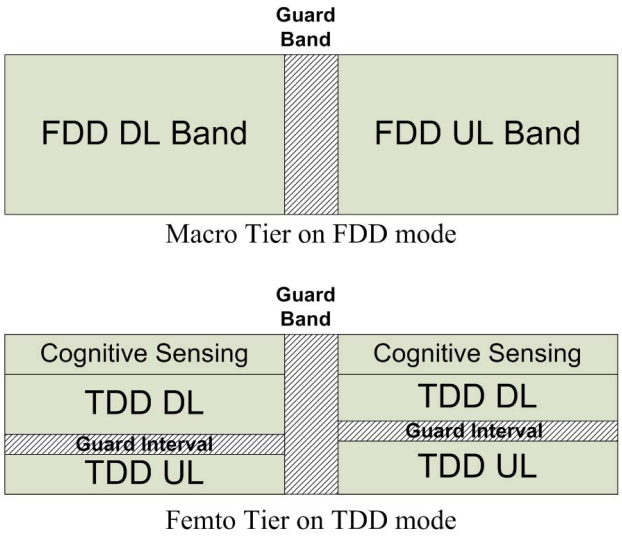

Fig. 1. Cognitive hybrid division duplex scheme.

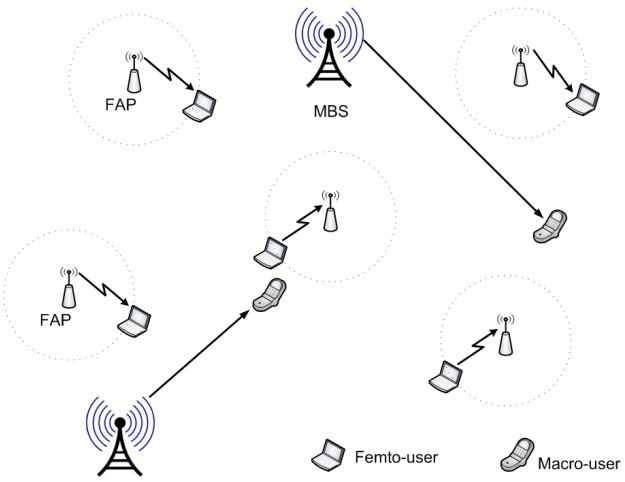

Fig. 2. Two-tier CHDD system when macro tier is in D mode.

We do not assume centralized control for the femtocell network and each femtocell is configured as d with probability q and u with probability $1-q$ in each time slot, where the configuration is independent across time slots and femtocells. For simplicity, we assume that this statistical mode multiplexing probability q is the same for all femtocells. Thus, the point processes $\Phi, \tilde{\Phi}$ are enriched with independent marks $\{f_1(t), f_2(t)...\}$ to form marked point processes

[2]These rates can be achieved by sending codewords at a fixed rate determined by the SINR threshold.

$\{(Y_i, f_i(t))\}_{i=1}^{\infty}$, $\{(Z_i, f_i(t))\}_{i=1}^{\infty}$. Here, $f_i(t)$ denotes the mode of the i-th femtocell at time t, with $\mathbb{P}(f_i(t) = \mathsf{d}) = q = 1 - \mathbb{P}(f_i(t) = \mathsf{u})$, which are independent across i and t. Thus, in each time slot t, the transmitting FAPs $\Phi^{\mathsf{d}}(t) = \{Y_i \in \Phi : f_i(t) = \mathsf{d}\} \sim \text{PPP}(q\lambda_{\mathrm{f}})$ and the transmitting femtocell users $\tilde{\Phi}^{\mathsf{u}}(t) = \left\{Z_i \in \tilde{\Phi} : f_i(t) = \mathsf{u}\right\} \sim \text{PPP}((1-q)\lambda_{\mathrm{f}})$. Now, at time slot t, the active sets of FAPs and femtocell users, namely Φ_t^{d} and $\tilde{\Phi}_t^{\mathsf{u}}$, are independent since the configurations of femtocells are independent. By marking a point in $Y_i \in \Phi$ either as d with probability q or u with probability $1-q$ independently, we see that $\Phi^{\mathsf{d}} = \{Y_i : \text{mark } = \mathsf{d}\}$ and $\Phi^{\mathsf{u}} = \{Y_j : \text{mark } = \mathsf{u}\}$ are two mutually independent PPPs. Finally, $\tilde{\Phi}^{\mathsf{u}} = \{Y_j + R_j : \text{mark of } Y_j = \mathsf{d}\}$ such that R_j is a random vector with distance R_{f}, is still a $\text{PPP}((1-q)\lambda_{\mathrm{f}})$ and $\tilde{\Phi}^{\mathsf{u}}$ is $\sigma(\Phi^{\mathsf{u}}, R_j)$-measurable. Thus, Φ_t^{d} and $\tilde{\Phi}_t^{\mathsf{u}}$ are independent since $\sigma(\Phi^{\mathsf{u}}, R_j)$ and $\sigma(\Phi^{\mathsf{d}})$ are independent by assumption.

When FAPs operate in closed access, only registered femtocell users can communicate with their FAPs. On the other hand, under open access FAP, a macrocell user can access both MBS and FAP as long as it is within the femtocell coverage area. Specifically, we consider the following two open access policies:

- *Location-based open access policy (LOAP)*, where macrocell user's communication is handed over from M to F, the nearest open access FAP operating in the same mode, if the ratio of the distance to that FAP to the distance of the nearest MBS falls below a threshold κ, i.e. if
$$\|\mathsf{F} - u\| < \kappa \|\mathsf{M} - u\|. \tag{2}$$
- *Distance-based open access policy (DOAP)*, where macrocell user's communication is handed over from M to F if the distance to the nearest FAP falls below a fixed threshold R_{HO}, i.e. if
$$\|\mathsf{F} - u\| < \mathrm{R}_{\mathsf{HO}}. \tag{3}$$

Both policies are illustrated in Fig. 3.

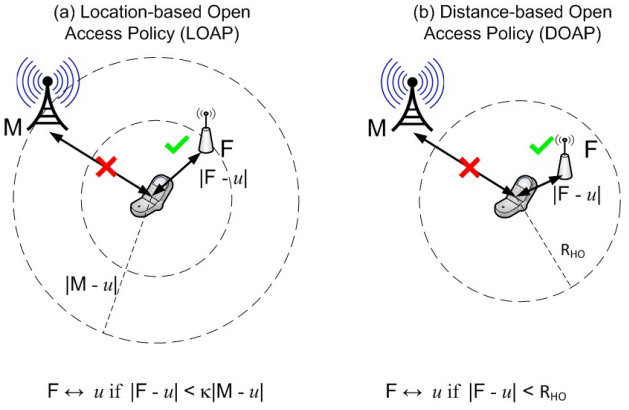

Fig. 3. Open access policy.

III. Performance Analysis

In this section, we evaluate the transmit success probability, the network throughput, and the spatial average capacity of a *typical* pair (x, u) of BS x and its associated user u.[3] By *typical*, we mean that we evaluate the statistics for a user located at, say, the origin. The statistics are independent of the location of the BS and user pair because the point processes are stationary. For notational convenience, the subscripts m and f denotes the macrocell and femtocell tier, respectively. Also, because all the statistics are independent across each time slot, the statistics are also true for any given time slot t. We shall omit t from our notation.

A. Macrocell in Downlink Mode

Firstly, let us consider the case where the FAPs operate in the macro-tier downlink (D) frequency band.

Theorem 1. *For the FAPs operating in the macro tier* D *frequency band, the macrocell transmit success probability* $\mathbb{P}_{\mathrm{m}}$ *and the femtocell transmit success probability* $\mathbb{P}_{\mathrm{f},\mathsf{D}}(\mathsf{D})(\leftrightarrow)$ *under CHDD scheme are, respectively, given by*

$$\begin{aligned}
&\mathbb{P}_{\mathrm{m}}(\mathsf{D}) \\
&= \frac{\lambda_{\mathrm{m}}}{\lambda_{\mathrm{m}} + \lambda_{\mathrm{m}}\rho(\gamma_{\mathrm{m}}, \alpha) + \lambda_{\mathrm{f}} D(q_{\mathsf{D}}) C(\alpha)(\gamma_{\mathrm{m}}/P_{\mathrm{m}})^{2/\alpha}} \qquad (4) \\
&\mathbb{P}_{\mathrm{f},\mathsf{D}}(\leftrightarrow) \\
&= q_{\mathsf{D}} \mathbb{P}_{\mathrm{f},\mathsf{D}}(\rightarrow) + (1 - q_{\mathsf{D}}) \mathbb{P}_{\mathrm{f},\mathsf{D}}(\leftarrow) \\
&= q_{\mathsf{D}} \exp\left(-\pi R_{\mathrm{f}}^2 \left(\lambda_{\mathrm{m}} P_{\mathrm{m}}^{2/\alpha} + \lambda_{\mathrm{f}} D(q_{\mathsf{D}})\right) C(\alpha) (\gamma_{\mathrm{f}}/P_{\mathrm{f}})^{2/\alpha}\right) \\
&+ (1 - q_{\mathsf{D}}) \exp\left(-\pi R_{\mathrm{f}}^2 \left(\lambda_{\mathrm{m}} P_{\mathrm{m}}^{2/\alpha} + \lambda_{\mathrm{f}} D(q_{\mathsf{D}})\right) C(\alpha) (\eta_{\mathrm{f}}/Q_{\mathrm{f}})^{2/\alpha}\right) \qquad (5)
\end{aligned}$$

where $D(q_{\mathsf{D}}) \triangleq q_{\mathsf{D}} P_{\mathrm{f}}^{2/\alpha} + (1 - q_{\mathsf{D}}) Q_{\mathrm{f}}^{2/\alpha}$, $\rho(\gamma_{\mathrm{m}}, \alpha) \triangleq \int_{\gamma_{\mathrm{m}}^{-2/\alpha}}^{\infty} \frac{\gamma_{\mathrm{m}}^{2/\alpha}}{1 + u^{\frac{\alpha}{2}}} \mathrm{d}u$, *and* $C(\alpha) \triangleq \frac{(2\pi)/\alpha}{\sin(2\pi/\alpha)}$.

Proof: See Appendix B. □

Remark 1. *Theorem 1 allows us to determine the optimal value of* $q_{\mathsf{D}}^{\star}$ *in several sub-cases. Firstly, let us obtain the optimal* $q_{\mathsf{D}}^{\star}$ *which maximizes the success probability in each tier.*

- *Since* $D(q_{\mathsf{D}})$ *is a linear function in* q_{D}*, the optimal* $q_{\mathsf{D},\mathrm{m}}^{\star}$ *that maximizes* (4) *alone is* 0 *(and* 1 *when* $Q_{\mathrm{f}} > P_{\mathrm{f}}$*).*
- *We remark that the optimal* $q_{\mathsf{D},\mathrm{f}}^{\star}$ *that optimizes* (5) *can be found by a numerical computation in the general case. For a range of parameters,* $q_{\mathsf{D},\mathrm{f}}^{\star}$ *takes a value in* $\{0, 1\}$*, following which* $q_{\mathsf{D},\mathrm{f}}^{\star}$ *is determined by:*
  1) *If* $F_{\mathsf{D}}(\gamma_{\mathrm{f}}, \eta_{\mathrm{f}}, P_{\mathrm{f}}, Q_{\mathrm{f}}) > 1$*, we have* $q_{\mathsf{D},\mathrm{f}}^{\star} = 1$.
  2) *If* $F_{\mathsf{D}}(\gamma_{\mathrm{f}}, \eta_{\mathrm{f}}, P_{\mathrm{f}}, Q_{\mathrm{f}}) < 1$*, we have* $q_{\mathsf{D},\mathrm{f}}^{\star} = 0$.
  3) *If* $F_{\mathsf{D}}(\gamma_{\mathrm{f}}, \eta_{\mathrm{f}}, P_{\mathrm{f}}, Q_{\mathrm{f}}) = 1$*, we have* $q_{\mathsf{D},\mathrm{f}}^{\star} = 0$ *or* 1*,*

  where $F_{\mathsf{D}}(\gamma_{\mathrm{f}}, \eta_{\mathrm{f}}, P_{\mathrm{f}}, Q_{\mathrm{f}}) \triangleq \left(\frac{\eta_{\mathrm{f}} P_{\mathrm{f}}}{\gamma_{\mathrm{f}} Q_{\mathrm{f}}}\right)^{2/\alpha} \left(\frac{\lambda_{\mathrm{m}} P_{\mathrm{m}}^{2/\alpha} + \lambda_{\mathrm{f}} Q_{\mathrm{f}}^{2/\alpha}}{\lambda_{\mathrm{m}} P_{\mathrm{m}}^{2/\alpha} + \lambda_{\mathrm{f}} P_{\mathrm{f}}^{2/\alpha}}\right)$*. One such range is given by* $P_{\mathrm{f}}/Q_{\mathrm{f}} > \gamma_{\mathrm{f}}/\eta_{\mathrm{f}}$ *(a transmit power constraint),* $\lambda_{\mathrm{f}} < \frac{(P_{\mathrm{f}}\eta_{\mathrm{f}})^{2/\alpha} - (Q_{\mathrm{f}}\gamma_{\mathrm{f}})^{2/\alpha}}{\eta_{\mathrm{f}}^{2/\alpha}\gamma_{\mathrm{f}}^{2/\alpha}(P_{\mathrm{f}}^{2/\alpha} - Q_{\mathrm{f}}^{2/\alpha})} \frac{1}{\pi R_{\mathrm{f}}^2 C(\alpha)}$ *(a FAP density constraint), and* $\exp\left(\pi R_{\mathrm{f}}^2 \left(\lambda_{\mathrm{m}} P_{\mathrm{m}}^{2/\alpha} + \lambda_{\mathrm{f}} Q_{\mathrm{f}}^{2/\alpha}\right) C(\alpha) \left(\left(\frac{\eta_{\mathrm{f}}}{Q_{\mathrm{f}}}\right)^{2/\alpha} - \left(\frac{\gamma_{\mathrm{f}}}{P_{\mathrm{f}}}\right)^{2/\alpha}\right)\right) > 1 + \pi R_{\mathrm{f}}^2 C(\alpha) (\eta_{\mathrm{f}}/Q_{\mathrm{f}})^{2/\alpha} \lambda_{\mathrm{f}} (P_{\mathrm{f}}^{2/\alpha} - Q_{\mathrm{f}}^{2/\alpha})$.

Next, we consider the following sub-cases.

[3] Our definition of transmit success probability is the same as coverage probability used in [11].

- *When $\lambda_{\mathrm{f}} \gg \lambda_{\mathrm{m}}$, (4) and (5) can be approximated as*

$$\mathbb{P}_{\mathrm{m}}(\mathsf{D}) \approx \frac{\lambda_{\mathrm{m}} P_{\mathrm{m}}^{2/\alpha}}{\lambda_{\mathrm{f}} D(q_{\mathsf{D}}) C(\alpha) \gamma_{\mathrm{m}}^{2/\alpha}} \tag{6}$$

$$\mathbb{P}_{\mathrm{f},\mathsf{D}}(\leftrightarrow) \approx (1-q_{\mathsf{D}}) \exp\left(-\pi R_{\mathrm{f}}^2 \lambda_{\mathrm{f}} D(q_{\mathsf{D}}) C(\alpha) (\eta_{\mathrm{f}}/Q_{\mathrm{f}})^{2/\alpha}\right) + q_{\mathsf{D}} \exp\left(-\pi R_{\mathrm{f}}^2 \lambda_{\mathrm{f}} D(q_{\mathsf{D}}) C(\alpha) (\gamma_{\mathrm{f}}/P_{\mathrm{f}})^{2/\alpha}\right). \tag{7}$$

From (6), $q_{\mathsf{D}} = 0$ maximizes $\mathbb{P}_{\mathrm{m}}(\mathsf{D})$. To determine the optimal $q_{\mathsf{D},\mathrm{f}}^{\star}$ that maximizes (7), we perform the same analysis as in the general cases, except that instead of evaluating $F_{\mathsf{D}}(\gamma_{\mathrm{f}}, \eta_{\mathrm{f}}, P_{\mathrm{f}}, Q_{\mathrm{f}})$, the following suffices:

1) *If $\eta_{\mathrm{f}}/\gamma_{\mathrm{f}} > 1$, we have $q_{\mathsf{D},\mathrm{f}}^{\star} = 1$.*
2) *If $\eta_{\mathrm{f}}/\gamma_{\mathrm{f}} < 1$, we have $q_{\mathsf{D},\mathrm{f}}^{\star} = 0$.*
3) *If $\eta_{\mathrm{f}}/\gamma_{\mathrm{f}} = 1$, we have $q_{\mathsf{D},\mathrm{f}}^{\star} = 0$ or 1.*

- *When $P_{\mathrm{m}} \gg P_{\mathrm{f}}$ and $P_{\mathrm{m}} \gg Q_{\mathrm{f}}$, we have*

$$\mathbb{P}_{\mathrm{m}}(\mathsf{D}) \approx \frac{1}{1+\rho(\gamma_{\mathrm{m}}, \alpha)} \tag{8}$$

$$\mathbb{P}_{\mathrm{f},\mathsf{D}}(\leftrightarrow) \approx (1-q_{\mathsf{D}}) \exp\left(-\pi R_{\mathrm{f}}^2 \lambda_{\mathrm{m}} C(\alpha) (P_{\mathrm{m}} \eta_{\mathrm{f}}/Q_{\mathrm{f}})^{2/\alpha}\right) + q_{\mathsf{D}} \exp\left(-\pi R_{\mathrm{f}}^2 \lambda_{\mathrm{m}} C(\alpha) (P_{\mathrm{m}} \gamma_{\mathrm{f}}/P_{\mathrm{f}})^{2/\alpha}\right) \tag{9}$$

From (8), we see that $\mathbb{P}_{\mathrm{m}}(\mathsf{D})$ does not depend on q_{D}, implying that the macro tier is completely unaffected by the interference from the femto tier. Expression (9) is a linear function increasing in q_{D} and so the optimal $q_{\mathsf{D},\mathrm{f}}^{\star}$ that maximizes (9) is 1, such that $\mathbb{P}_{\mathrm{f},\mathsf{D}}^{\mathrm{opt}}(\leftrightarrow) \approx \exp\left(-\pi R_{\mathrm{f}}^2 \lambda_{\mathrm{m}} P_{\mathrm{m}}^{2/\alpha} C(\alpha) (\gamma_{\mathrm{f}}/P_{\mathrm{f}})^{2/\alpha}\right)$. Therefore, it is optimal for all cognitive femtocells to operate in the D mode.

- *In general, to ensure that we do not over-deploy cognitive femtocells and cause performance degradation to the macro tier, we need to have some form of QoS guarantee for the macro tier while controlling the intensity of the deployed FAPs. By using Theorem 1, we can determine the maximal intensity of cognitive FAPs that can be deployed within the macro tier and still satisfy $\mathbb{P}_{\mathrm{m}}(\mathsf{D}) \geq \epsilon$, where $\epsilon \in (0,1]$. For a given λ_{m} and q_{D}, the maximal $\lambda_{\mathrm{f}}^{\star}$ can be determined using (4) as follows:*

$$\lambda_{\mathrm{f}}^{\star} = \left(1/\epsilon - 1 - \rho(\gamma_{\mathrm{m}}, \alpha)\right) \frac{\lambda_{\mathrm{m}} P_{\mathrm{m}}^{2/\alpha}}{C(\alpha) \gamma_{\mathrm{m}}^{2/\alpha} D(q_{\mathsf{D}})} \tag{10}$$

and the corresponding femtocell transmit success probability in (5) becomes

$$\mathbb{P}_{\mathrm{f},\mathsf{D}}(\leftrightarrow) = (1-q_{\mathsf{D}}) \exp\left[-\pi R_{\mathrm{f}}^2 \lambda_{\mathrm{m}} \left(\frac{P_{\mathrm{m}} \eta_{\mathrm{f}}}{Q_{\mathrm{f}}}\right)^{2/\alpha} C_{\mathsf{D}}\right] + q_{\mathsf{D}} \exp\left[-\pi R_{\mathrm{f}}^2 \lambda_{\mathrm{m}} \left(\frac{P_{\mathrm{m}} \gamma_{\mathrm{f}}}{P_{\mathrm{f}}}\right)^{2/\alpha} C_{\mathsf{D}}\right] \tag{11}$$

where $C_{\mathsf{D}} = C(\alpha) + \gamma_{\mathrm{m}}^{-2/\alpha}(1/\epsilon - 1 - \rho(\gamma_{\mathrm{m}}, \alpha))$.

For macro tier in D mode, the total network throughput under CHDD scheme can be written as

$$\mathcal{T}_{\mathsf{D}}(q_{\mathsf{D}}) = \lambda_{\mathrm{m}} \mathbb{P}_{\mathrm{m}}(\mathsf{D}) \log(1+\gamma_{\mathrm{m}}) + q_{\mathsf{D}} \lambda_{\mathrm{f}} \mathbb{P}_{\mathrm{f},\mathsf{D}}(\rightarrow) \log(1+\gamma_{\mathrm{f}}) + (1-q_{\mathsf{D}}) \lambda_{\mathrm{f}} \mathbb{P}_{\mathrm{f},\mathsf{D}}(\leftarrow) \log(1+\eta_{\mathrm{f}}). \tag{12}$$

Theorem 2. *For macro tier in D mode, the macrocell and femtocell spatial average capacities under CHDD scheme are, respectively, given by*

$$R_{\mathrm{m}}(\mathsf{D}) = \int_{t=0}^{\infty} \frac{\lambda_{\mathrm{m}}}{\lambda_{\mathrm{m}} + \lambda_{\mathrm{m}} \rho(e^t - 1, \alpha) + \lambda_{\mathrm{f}} D(q_{\mathsf{D}}) C(\alpha) (\frac{e^t - 1}{P_{\mathrm{m}}})^{2/\alpha}} \mathrm{d}t \tag{13}$$

$$R_{\mathrm{f},\mathsf{D}}(\leftrightarrow) = q_{\mathsf{D}} \int_{t=0}^{\infty} \exp\Big(-\pi R_{\mathrm{f}}^2 \left(\lambda_{\mathrm{m}} P_{\mathrm{m}}^{2/\alpha} + \lambda_{\mathrm{f}} D(q_{\mathsf{D}})\right) \times C(\alpha) ((e^t - 1)/P_{\mathrm{f}})^{2/\alpha}\Big) \mathrm{d}t + (1-q_{\mathsf{D}}) \int_{t=0}^{\infty} \exp\Big(-\pi R_{\mathrm{f}}^2 \left(\lambda_{\mathrm{m}} P_{\mathrm{m}}^{2/\alpha} + \lambda_{\mathrm{f}} D(q_{\mathsf{D}})\right) \times C(\alpha) ((e^t - 1)/Q_{\mathrm{f}})^{2/\alpha}\Big) \mathrm{d}t. \tag{14}$$

In the case where $\alpha = 4$, we get simplifications of the above expressions given by

$$R_{\mathrm{m},\mathsf{D},\alpha=4} = \int_{z=0}^{\infty} \frac{2\lambda_{\mathrm{m}}}{\lambda_{\mathrm{m}} + \lambda_{\mathrm{m}} z \tan^{-1} z + \lambda_{\mathrm{f}} D(q_{\mathsf{D}}) z \frac{C(\alpha)}{\sqrt{P_{\mathrm{m}}}}} \frac{z}{z^2+1} \mathrm{d}z \tag{15}$$

$$R_{\mathrm{f},\mathsf{D},\alpha=4}(\leftrightarrow) = q_{\mathsf{D}}(\pi \sin A_1 - 2\mathrm{Si}(A_1) \sin A_1 - 2\mathrm{Ci}(A_1) \cos A_1) + (1-q_{\mathsf{D}})(\pi \sin A_2 - 2\mathrm{Si}(A_2) \sin A_2 - 2\mathrm{Ci}(A_2) \cos A_2) \tag{16}$$

where $A_1 = \frac{\pi^2 R_{\mathrm{f}}^2}{2\sqrt{P_{\mathrm{f}}}} \left(\lambda_{\mathrm{m}} \sqrt{P_{\mathrm{m}}} + \lambda_{\mathrm{f}} D(q_{\mathsf{D}})\right)$ and $A_2 = \frac{\pi^2 R_{\mathrm{f}}^2}{2\sqrt{Q_{\mathrm{f}}}} \left(\lambda_{\mathrm{m}} \sqrt{P_{\mathrm{m}}} + \lambda_{\mathrm{f}} D(q_{\mathsf{D}})\right)$. In addition, Si and Ci are trigonometric integral functions defined as $\mathrm{Si}(z) = \int_0^z \frac{\sin t}{t} \mathrm{d}t$ and $\mathrm{Ci}(z) = -\int_z^{\infty} \frac{\cos t}{t} \mathrm{d}t$, respectively.

Proof: See Appendix D. □

We now consider the case where the CHDD scheme operates open access (see Theorem 3).

B. Macrocell in uplink mode

Next, we consider that all the macrocells are in U mode and derive similar performance measures as in the D mode case.

Theorem 4. *For macro tier in U mode, the macrocell transmit success probability $\mathbb{P}_{\mathrm{m}}(\mathsf{U})$ and femtocell transmit success probability $\mathbb{P}_{\mathrm{f},\mathsf{U}}(\leftrightarrow)$ under CHDD scheme in any given time slot are, respectively, given by*

$$\mathbb{P}_{\mathrm{m}}(\mathsf{U}) = \frac{\lambda_{\mathrm{m}}}{\lambda_{\mathrm{m}} + \left(\mu_{\mathrm{m}} + \left(1/Q_{\mathrm{m}}\right)^{2/\alpha} \lambda_{\mathrm{f}} D(q_{\mathsf{U}})\right) C(\alpha) \eta_{\mathrm{m}}^{2/\alpha}} \tag{19}$$

$$\mathbb{P}_{\mathrm{f},\mathsf{U}}(\leftrightarrow) = (1-q_{\mathsf{U}}) \exp(-\pi R_{\mathrm{f}}^2 \left(\mu_{\mathrm{m}} Q_{\mathrm{m}}^{2/\alpha} + \lambda_{\mathrm{f}} D(q_{\mathsf{U}})\right) C(\alpha) (\eta_{\mathrm{f}}/Q_{\mathrm{f}})^{2/\alpha}) + q_{\mathsf{U}} \exp(-\pi R_{\mathrm{f}}^2 \left(\mu_{\mathrm{m}} Q_{\mathrm{m}}^{2/\alpha} + \lambda_{\mathrm{f}} D(q_{\mathsf{U}})\right) C(\alpha) (\gamma_{\mathrm{f}}/P_{\mathrm{f}})^{2/\alpha}). \tag{20}$$

Proof: See Appendix F. □

Theorem 3. *In the following, we give the macrocell transmit success probability when the macro tier is in* D *mode and open access FAP. In the case where we operate the Location-based open access policy (LOAP), the success probability is given by*

$$\mathbb{P}_{\mathrm{m,o1}}(\mathsf{D}) = \frac{\lambda_{\mathrm{m}}}{\lambda_{\mathrm{m}}(1+\rho(\gamma_{\mathrm{m}},\alpha)) + \kappa^2 q_{\mathsf{D}}\lambda_{\mathrm{f}}(1+\rho(\gamma_{\mathrm{m}}P_{\mathrm{f}}/\kappa^{\alpha}P_{\mathrm{m}},\alpha)) + (1-q_{\mathsf{D}})\lambda_{\mathrm{f}}(Q_{\mathrm{f}}\gamma_{\mathrm{m}}/P_{\mathrm{m}})^{2/\alpha}C(\alpha)} + \frac{q_{\mathsf{D}}\lambda_{\mathrm{f}}}{(1/\kappa^2)\lambda_{\mathrm{m}}(1+\rho(\gamma_{\mathrm{f}}P_{\mathrm{m}}\kappa^{\alpha}/P_{\mathrm{f}},\alpha)) + q_{\mathsf{D}}\lambda_{\mathrm{f}}(1+\rho(\gamma_{\mathrm{f}},\alpha)) + (1-q_{\mathsf{D}})\lambda_{\mathrm{f}}(Q_{\mathrm{f}}\gamma_{\mathrm{f}}/P_{\mathrm{f}})^{2/\alpha}C(\alpha)}, \tag{17}$$

and as for the case where we operate under the distance-based open access policy (DOAP), the success probability is given by

$$\begin{aligned}\mathbb{P}_{\mathrm{m,o2}}(\mathsf{D}) \;=\; & \frac{q_{\mathsf{D}}\lambda_{\mathrm{f}}(1-\exp(-\pi R_{\mathsf{HO}}^2(q_{\mathsf{D}}\lambda_{\mathrm{f}}(1+\rho(\gamma_{\mathrm{f}},\alpha)) + (\lambda_{\mathrm{m}}P_{\mathrm{m}}^{2/\alpha} + (1-q_{\mathsf{D}})\lambda_{\mathrm{f}}Q_{\mathrm{f}}^{2/\alpha})(\gamma_{\mathrm{f}}/P_{\mathrm{f}})^{2/\alpha}C(\alpha))))}{q_{\mathsf{D}}\lambda_{\mathrm{f}}(1+\rho(\gamma_{\mathrm{f}},\alpha)) + (\lambda_{\mathrm{m}}P_{\mathrm{m}}^{2/\alpha} + (1-q_{\mathsf{D}})\lambda_{\mathrm{f}}Q_{\mathrm{f}}^{2/\alpha})(\gamma_{\mathrm{f}}/P_{\mathrm{f}})^{2/\alpha}C(\alpha)} \\ & + \exp(-\pi R_{\mathsf{HO}}^2 q_{\mathsf{D}}\lambda_{\mathrm{f}})\int_{s=0}^{\infty}\exp(-\pi s^2\lambda_{\mathrm{m}}\rho(\gamma_{\mathrm{m}},\alpha))\exp(-\pi s^2(1-q_{\mathsf{D}})\lambda_{\mathrm{f}}(Q_{\mathrm{f}}\gamma_{\mathrm{m}}/P_{\mathrm{m}})^{2/\alpha}C(\alpha)) \\ & \exp(-\pi s^2 q_{\mathsf{D}}\lambda_{\mathrm{f}}(\gamma_{\mathrm{m}}P_{\mathrm{f}}/P_{\mathrm{m}})^{2/\alpha}\int_{S_0}^{\infty}1/(1+z^{\alpha/2})dz)2\pi\lambda_{\mathrm{m}}s\exp(-\pi\lambda_{\mathrm{m}}s^2)ds\end{aligned} \tag{18}$$

where $S_0 = \frac{R_{\mathsf{HO}}^2}{s^2}\left(\frac{P_{\mathrm{m}}}{P_{\mathrm{f}}\gamma_{\mathrm{m}}}\right)^{2/\alpha}$.

Proof: See Appendix E. □

Remark 2. *The analysis is similar to the case where the macro tier is in* D *mode. Firstly, let us obtain the optimal* $q_{\mathsf{U}}^{\star}$ *that maximizes the success probability in each tier.*

- *Since* $D(q_{\mathsf{U}})$ *is a linear function in* q_{U}*, the optimal* $q_{\mathsf{U},\mathrm{m}}^{\star}$ *that maximizes* (4) *alone is* 0 *(and* 1 *when* $Q_{\mathrm{f}} > P_{\mathrm{f}}$*).*
- *If we have the parameter constraints* $P_{\mathrm{f}}/Q_{\mathrm{f}} > \gamma_{\mathrm{f}}/\eta_{\mathrm{f}}$ *and* $\lambda_{\mathrm{f}} < \frac{(P_{\mathrm{f}}\eta_{\mathrm{f}})^{2/\alpha}-(Q_{\mathrm{f}}\gamma_{\mathrm{f}})^{2/\alpha}}{\eta_{\mathrm{f}}^{2/\alpha}\gamma_{\mathrm{f}}^{2/\alpha}(P_{\mathrm{f}}^{2/\alpha}-Q_{\mathrm{f}}^{2/\alpha})}\frac{1}{\pi R_{\mathrm{f}}^2 C(\alpha)}$ *then the following is a sufficient condition for the optimal* $q_{\mathsf{U},\mathrm{f}}^{\star}$ *that optimizes* (5) *to be* $\in \{0,1\}$*:* $\exp\big(\pi R_{\mathrm{f}}^2\big(\mu_{\mathrm{m}}P_{\mathrm{m}}^{2/\alpha} + \lambda_{\mathrm{f}}Q_{\mathrm{f}}^{2/\alpha}\big)C(\alpha)\big(\big(\frac{\eta_{\mathrm{f}}}{Q_{\mathrm{f}}}\big)^{2/\alpha} - \big(\frac{\gamma_{\mathrm{f}}}{P_{\mathrm{f}}}\big)^{2/\alpha}\big)\big) > 1+\pi R_{\mathrm{f}}^2 C(\alpha)(\eta_{\mathrm{f}}/Q_{\mathrm{f}})^{2/\alpha}\lambda_{\mathrm{f}}(P_{\mathrm{f}}^{2/\alpha}-Q_{\mathrm{f}}^{2/\alpha})$*, following which, the optimal* $q_{\mathsf{U},\mathrm{f}}^{\star}$ *is given by*
  1) *If* $F_{\mathsf{U}}(\gamma_{\mathrm{f}},\eta_{\mathrm{f}},P_{\mathrm{f}},Q_{\mathrm{f}}) > 1$*, we have* $q_{\mathsf{U},\mathrm{f}}^{\star} = 1$*.*
  2) *If* $F_{\mathsf{U}}(\gamma_{\mathrm{f}},\eta_{\mathrm{f}},P_{\mathrm{f}},Q_{\mathrm{f}}) < 1$*, we have* $q_{\mathsf{U},\mathrm{f}}^{\star} = 0$*.*
  3) *If* $F_{\mathsf{U}}(\gamma_{\mathrm{f}},\eta_{\mathrm{f}},P_{\mathrm{f}},Q_{\mathrm{f}}) = 1$*, we have* $q_{\mathsf{U},\mathrm{f}}^{\star} = 0$ *or* 1*.*

  where $F_{\mathsf{U}}(\gamma_{\mathrm{f}},\eta_{\mathrm{f}},P_{\mathrm{f}},Q_{\mathrm{f}}) \triangleq \big(\frac{\eta_{\mathrm{f}}P_{\mathrm{f}}}{\gamma_{\mathrm{f}}Q_{\mathrm{f}}}\big)^{2/\alpha}\Big(\frac{\mu_{\mathrm{m}}Q_{\mathrm{m}}^{2/\alpha}+\lambda_{\mathrm{f}}Q_{\mathrm{f}}^{2/\alpha}}{\mu_{\mathrm{m}}Q_{\mathrm{m}}^{2/\alpha}+\lambda_{\mathrm{f}}P_{\mathrm{f}}^{2/\alpha}}\Big)$*. The proofs of the statements are similar to the case where the macrocell is in* D*.*

Next we consider the following sub-cases:

- *When* $\lambda_{\mathrm{f}} \gg \mu_{\mathrm{m}}$*,* (19) *and* (20) *can be approximated as*

$$\mathbb{P}_{\mathrm{m}}(\mathsf{U}) \approx \frac{\lambda_{\mathrm{m}}}{\lambda_{\mathrm{m}} + (1/Q_{\mathrm{m}})^{2/\alpha}\lambda_{\mathrm{f}}D(q_{\mathsf{U}})C(\alpha)\eta_{\mathrm{m}}^{2/\alpha}} \tag{21}$$

$$\mathbb{P}_{\mathrm{f,U}}(\leftrightarrow) \approx (1-q_{\mathsf{U}})\exp(-\pi R_{\mathrm{f}}^2\lambda_{\mathrm{f}}D(q_{\mathsf{U}})C(\alpha)(\eta_{\mathrm{f}}/Q_{\mathrm{f}})^{2/\alpha}) + q_{\mathsf{U}}\exp(-\pi R_{\mathrm{f}}^2\lambda_{\mathrm{f}}D(q_{\mathsf{U}})C(\alpha)(\gamma_{\mathrm{f}}/P_{\mathrm{f}})^{2/\alpha}). \tag{22}$$

  From (21)*, we can observe that* $\mathbb{P}_{\mathrm{m}}(\mathsf{U})$ *decreases with increasing* q_{U} *so the optimal* $q_{\mathsf{U},\mathrm{f}}^{\star}$ *that maximizes* $\mathbb{P}_{\mathrm{m}}(\mathsf{U})$ *is* 0*. Next, we see that* (22) *is the same as* (7) *and thus the optimal* $q_{\mathsf{U},\mathrm{f}}^{\star}$ *that maximizes* $\mathbb{P}_{\mathrm{f,U}}(\leftrightarrow)$ *is the same* $q_{\mathsf{D},\mathrm{f}}^{\star}$ *that maximizes* (7)*.*
- *By using Theorem 4, we can determine the maximal intensity of cognitive FAPs to be deployed within the macro tier and still satisfy* $\mathbb{P}_{\mathrm{m}}(\mathsf{U}) \geq \epsilon$*, where* $\epsilon \in (0,1]$*. For a given* λ_{m}*,* μ_{m}*, and* q_{U}*, the maximal* $\lambda_{\mathrm{f}}^{\star}$ *is given as follows:*

$$\lambda_{\mathrm{f}}^{\star} = \left[\frac{1}{\epsilon} - 1 - \frac{\mu_{\mathrm{m}}}{\lambda_{\mathrm{m}}}C(\alpha)\eta_{\mathrm{m}}^{2/\alpha}\right]\frac{\lambda_{\mathrm{m}}Q_{\mathrm{m}}^{2/\alpha}}{C(\alpha)\eta_{\mathrm{m}}^{2/\alpha}D(q_{\mathsf{U}})} \tag{23}$$

  and the corresponding femtocell transmit success probability in (20) *becomes*

$$\mathbb{P}_{\mathrm{f,D}}(\leftrightarrow) \;=\; (1-q_{\mathsf{U}})\exp\left[-\pi R_{\mathrm{f}}^2\left(\frac{Q_{\mathrm{m}}\eta_{\mathrm{f}}}{Q_{\mathrm{f}}}\right)^{2/\alpha}C_{\mathsf{U}}\right] + q_{\mathsf{U}}\exp\left[-\pi R_{\mathrm{f}}^2\left(\frac{Q_{\mathrm{m}}\gamma_{\mathrm{f}}}{P_{\mathrm{f}}}\right)^{2/\alpha}C_{\mathsf{U}}\right] \tag{24}$$

  where $C_{\mathsf{U}} = \mu_{\mathrm{m}}C(\alpha) + \frac{\lambda_{\mathrm{m}}}{\eta_{\mathrm{m}}^{2/\alpha}}\big(\frac{1}{\epsilon} - 1 - \frac{\mu_{\mathrm{m}}}{\lambda_{\mathrm{m}}}C(\alpha)\eta_{\mathrm{m}}^{2/\alpha}\big)$*.*

Similarly to (12), the total network throughput under CHDD scheme in any given time slot t for macro tier in U mode is given by

$$\begin{aligned}\mathcal{T}_{\mathsf{U}}(q_{\mathsf{U}}) \;=\; & \mu_{\mathrm{m}}\mathbb{P}_{\mathrm{m}}(\mathsf{U})\log(1+\eta_{\mathrm{m}}) + q\lambda_{\mathrm{f}}\mathbb{P}_{\mathrm{f,U}}(\rightarrow)\log(1+\gamma_{\mathrm{f}}) \\ & +(1-q_{\mathsf{U}})\lambda_{\mathrm{f}}\mathbb{P}_{\mathrm{f,U}}(\leftarrow)\log(1+\eta_{\mathrm{f}}).\end{aligned} \tag{25}$$

Theorem 5. *For macro tier in* U *mode, the macrocell and femtocell spatial average capacities under CHDD scheme in any given time slot are, respectively, given by*

$$R_{\mathrm{m}}(\mathsf{U}) = \int_{t=0}^{\infty}\frac{\lambda_{\mathrm{m}}\mathrm{d}t}{\lambda_{\mathrm{m}} + \big(\mu_{\mathrm{m}} + \big(\frac{1}{Q_{\mathrm{m}}}\big)^{2/\alpha}\lambda_{\mathrm{f}}D(q_{\mathsf{U}})\big)C(\alpha)(e^t-1)^{2/\alpha}} \tag{26}$$

$$\begin{aligned}R_{\mathrm{f,U}} \;=\; & q\int_{t=0}^{\infty}\exp\Big(-\pi R_{\mathrm{f}}^2\big(\mu_{\mathrm{m}}Q_{\mathrm{m}}^{2/\alpha} + \lambda_{\mathrm{f}}D(q_{\mathsf{U}})\big) \\ & \qquad C(\alpha)((e^t-1)/P_{\mathrm{f}})^{2/\alpha}\Big)\mathrm{d}t \\ & +(1-q_{\mathsf{U}})\int_{t=0}^{\infty}\exp\Big(-\pi R_{\mathrm{f}}^2\big(\mu_{\mathrm{m}}Q_{\mathrm{m}}^{2/\alpha} + \lambda_{\mathrm{f}}D(q_{\mathsf{U}})\big) \\ & \qquad C(\alpha)((e^t-1)Q_{\mathrm{f}})^{2/\alpha}\Big)\mathrm{d}t.\end{aligned} \tag{27}$$

Simplifications of the above expressions in the case where $\alpha = 4$ are given by

$$R_{\mathrm{m},\mathsf{U},\alpha=4} = \frac{2\lambda_{\mathrm{m}}^2(\log\lambda_{\mathrm{m}} - \log B_{\mathsf{U}}) + \lambda_{\mathrm{m}} B_{\mathsf{U}}\pi}{\lambda_{\mathrm{m}}^2 + B_{\mathsf{U}}^2} \quad (28)$$

$$\begin{aligned} R_{\mathrm{f},\mathsf{U},\alpha=4}(\leftrightarrow) = {} & q_{\mathsf{U}}(\pi\sin A_3 - 2\mathrm{Si}(A_3)\sin A_3 \\ & -2\mathrm{Ci}(A_3)\cos A_3) + (1-q_{\mathsf{U}})(\pi\sin A_4 \\ & -2\mathrm{Si}(A_4)\sin A_4 - 2\mathrm{Ci}(A_4)\cos A_4) \end{aligned} \quad (29)$$

where $A_3 = \frac{\pi^2 R_{\mathrm{f}}^2}{2\sqrt{P_{\mathrm{f}}}}\big(\lambda_{\mathrm{m}}\sqrt{Q_{\mathrm{m}}} + q_{\mathsf{U}}\lambda_{\mathrm{f}}\sqrt{P_{\mathrm{f}}} + (1-q_{\mathsf{U}})\lambda_{\mathrm{f}}\sqrt{Q_{\mathrm{f}}}\big)$, $A_4 = \frac{\pi^2 R_{\mathrm{f}}^2}{2\sqrt{Q_{\mathrm{f}}}}\big(\lambda_{\mathrm{m}}\sqrt{Q_{\mathrm{m}}} + q_{\mathsf{U}}\lambda_{\mathrm{f}}\sqrt{P_{\mathrm{f}}} + (1-q_{\mathsf{U}})\lambda_{\mathrm{f}}\sqrt{Q_{\mathrm{f}}}\big)$, *and* $B_{\mathsf{U}} = \big(\mu_{\mathrm{m}} + q_{\mathsf{U}}\lambda_{\mathrm{f}}\sqrt{\frac{P_{\mathrm{f}}}{Q_{\mathrm{m}}}} + (1-q_{\mathsf{U}})\lambda_{\mathrm{f}}\sqrt{\frac{Q_{\mathrm{f}}}{Q_{\mathrm{m}}}}\big)(\pi/2)$.

Proof: See Appendix B. □

Just like we did in the case when Macro is in downlink, we implement open access in the case when Macro is in uplink (see Theorem 6).

IV. Optimization of CHDD Scheme

In this section, we employ the analytical results derived in the previous section in order to formulate and solve different network performance-related problems.

A. Macrocell in downlink mode

Consider the total network throughput maximization problem with a macro tier QoS constraint as follows:

$$\mathcal{P}_{\mathsf{D}} : \begin{cases} \max\limits_{q_{\mathsf{D}}} & \mathcal{T}_{\mathsf{D}}(q_{\mathsf{D}}) \\ \text{s.t.} & \mathbb{P}_{\mathrm{m}}(\mathsf{D}) \geq \epsilon_{\mathsf{D}} \end{cases} \quad (32)$$

where $\epsilon_{\mathsf{D}} \in (0,1]$ and $\mathcal{T}_{\mathsf{D}}(q_{\mathsf{D}})$ can be obtained by substituting (4) and (5) into (12) to obtain

$$\begin{aligned} & \mathcal{T}_{\mathsf{D}}(q_{\mathsf{D}}) \\ = {} & \frac{\lambda_{\mathrm{m}}\log(1+\gamma_{\mathrm{m}})}{1+\rho(\gamma_{\mathrm{m}},\alpha) + (1/P_{\mathrm{m}}^{2/\alpha})(1/\lambda_{\mathrm{m}})\lambda_{\mathrm{f}} D(q_{\mathsf{D}}) C(\alpha)\gamma_{\mathrm{m}}^{2/\alpha}} \\ & + \exp\big(-\pi R_{\mathrm{f}}^2\big(\lambda_{\mathrm{m}}P_{\mathrm{m}}^{2/\alpha} + \lambda_{\mathrm{f}}D(q_{\mathsf{D}})\big)C(\alpha)(\gamma_{\mathrm{f}}/P_{\mathrm{f}})^{2/\alpha}\big) \\ & \qquad \times q_{\mathsf{D}}\lambda_{\mathrm{f}}\log(1+\gamma_{\mathrm{f}}) \\ & + \exp\big(-\pi R_{\mathrm{f}}^2\big(\lambda_{\mathrm{m}}P_{\mathrm{m}}^{2/\alpha} + \lambda_{\mathrm{f}}D(q_{\mathsf{D}})\big)C(\alpha)(\eta_{\mathrm{f}}/Q_{\mathrm{f}})^{2/\alpha}\big) \\ & \qquad \times (1-q_{\mathsf{D}})\lambda_{\mathrm{f}}\log(1+\eta_{\mathrm{f}}). \end{aligned} \quad (33)$$

Our previous analysis has shown that in many cases, the optimal value $q_{\mathsf{D}}^\star$ takes either 0 or 1. Moreover, we see that in many of our plots, the success probability is monotone in q for both macro and femto layer. We build on these observations to help us in the optimization. When the optimal value of $q_{\mathsf{D}}^\star$ is opposite in the macro and femto tiers, for example, 0 and 1 respectively, then intuitively, we would want to satisfy the QoS constraint tightly and solve for $q_{\mathsf{D}}^\star$.

We can make this more precise: Suppose $\lambda_{\mathrm{f}} \gg \lambda_{\mathrm{m}}$, $q_{\mathsf{D}}^\star$ is 0 and 1 for the macro and femto tier respectively, and the coverage rate for the femto tier increases monotonically with q_{D}, then the optimal solution to the maximization problem has an easy characterization. Because $\lambda_{\mathrm{f}} \gg \lambda_{\mathrm{m}}$, we essentially only optimize the sum of the second and third term in (33). In this case, we have

$$q_{\mathsf{D},0}^\star = \frac{\big(1/\epsilon_{\mathsf{D}} - 1 - \rho(\gamma_{\mathrm{m}},\alpha)\big)\lambda_{\mathrm{m}}P_{\mathrm{m}}^{2/\alpha}}{\big(P_{\mathrm{f}}^{2/\alpha} - Q_{\mathrm{f}}^{2/\alpha}\big)C(\alpha)\gamma_{\mathrm{m}}^{2/\alpha}\lambda_{\mathrm{f}}} - \frac{Q_{\mathrm{f}}^{2/\alpha}}{P_{\mathrm{f}}^{2/\alpha} - Q_{\mathrm{f}}^{2/\alpha}} \quad (34)$$

Now the optimal q that solves $\mathcal{P}_{\mathsf{D}}$ must satisfy the QoS constraint tightly. If $q_{\mathsf{D},0}^\star \geq 0$, then we have a feasible solution $q_{\mathsf{D}}^\star = \min\{1, q_{\mathsf{D},0}^\star\}$. The optimal total network throughput $\mathcal{T}_{\mathsf{D}}(q_{\mathsf{D}}^\star)$ may be found by substituting (34) into (33). Note that if $q_{\mathsf{D},0}^\star < 0$, then the QoS constraint needs to be further relaxed by lowering ϵ_{D}. This problem can be similarly extended to the case when we have $q_{\mathsf{D}}^\star$ equal to 1 and 0 for the macro and femto layer respectively, and the coverage rate for the femto tier decreases with q_{D}.

The above conditions can relaxed to broader cases where the above observations hold. The optimal $q_{\mathsf{D}}^\star$ which maximizes (34) can be obtained via a numerical computation for the most general case.

B. Macrocell in uplink mode

Similarly, the total network throughput maximization problem with a QoS constraint is given by

$$\mathcal{P}_{\mathsf{U}} : \begin{cases} \max\limits_{q_{\mathsf{U}}} & \mathcal{T}_{\mathsf{U}}(q_{\mathsf{U}}) \\ \text{s.t.} & \mathbb{P}_{\mathrm{m}}(\mathsf{U}) \geq \epsilon_{\mathsf{U}} \end{cases} \quad (35)$$

where $\epsilon_{\mathsf{U}} \in (0,1]$ and $\mathcal{T}_{\mathsf{U}}(q_{\mathsf{U}})$ can be written as

$$\begin{aligned} & \mathcal{T}_{\mathsf{U}}(q_{\mathsf{U}}) \\ & = \frac{\lambda_{\mathrm{m}}\mu_{\mathrm{m}}\log(1+\eta_{\mathrm{m}})}{\lambda_{\mathrm{m}} + \Big(\mu_{\mathrm{m}} + \lambda_{\mathrm{f}}(D(q_{\mathsf{U}})/Q_{\mathrm{m}}^{2/\alpha})\Big)C(\alpha)\eta_{\mathrm{m}}^{2/\alpha}} \\ & + \exp\Big(-\pi R_{\mathrm{f}}^2\Big(\mu_{\mathrm{m}}Q_{\mathrm{m}}^{2/\alpha} + \lambda_{\mathrm{f}}D(q_{\mathsf{U}})\Big)C(\alpha)(\gamma_{\mathrm{f}}/P_{\mathrm{f}})^{2/\alpha}\Big) \\ & \qquad \lambda_{\mathrm{f}}\log(1+\gamma_{\mathrm{f}})q_{\mathsf{U}} \\ & + \exp\Big(-\pi R_{\mathrm{f}}^2\Big(\mu_{\mathrm{m}}Q_{\mathrm{m}}^{2/\alpha} + \lambda_{\mathrm{f}}D(q_{\mathsf{U}})\Big)C(\alpha)(\eta_{\mathrm{f}}/Q_{\mathrm{f}})^{2/\alpha}\Big) \\ & \qquad \lambda_{\mathrm{f}}\log(1+\eta_{\mathrm{f}})(1-q_{\mathsf{U}}). \end{aligned} \quad (36)$$

The conditions for which we can have a simple characterization of the optimal throughput subject to the constraint are identical to the case where the macro tier is in D mode, namely: $\lambda_{\mathrm{f}} \gg \lambda_{\mathrm{m}}$, $\gamma_{\mathrm{f}} = \gamma_{\mathrm{f}}$, $q_{\mathsf{U}}^\star$ taking 0 and 1 for the macro and femto tier alone, respectively, and the coverage rate of the femto tier increases monotonically with q_{U}. Again, by satisfying the QoS constraint tightly, we get $q_{\mathsf{U},0}^\star$ for a given λ_{m}, μ_{m}, and λ_{f}:

$$q_{\mathsf{U},0}^\star = \frac{\lambda_{\mathrm{m}}/\epsilon_{\mathsf{U}} - \lambda_{\mathrm{m}} - \mu_{\mathrm{m}}C(\alpha)\eta_{\mathrm{m}}^{2/\alpha}}{\big(P_{\mathrm{f}}^{2/\alpha} - Q_{\mathrm{f}}^{2/\alpha}\big)Q_{\mathrm{m}}^{-2/\alpha}C(\alpha)\eta_{\mathrm{m}}^{2/\alpha}\lambda_{\mathrm{f}}} - \frac{Q_{\mathrm{f}}^{2/\alpha}}{P_{\mathrm{f}}^{2/\alpha} - Q_{\mathrm{f}}^{2/\alpha}} \quad (37)$$

where $q_{\mathsf{U}}^\star = \min\{1, q_{\mathsf{U},0}^\star\}$ if $q_{\mathsf{U},0}^\star > 0$. The optimal total network throughput $\mathcal{T}_{\mathsf{U}}(q_{\mathsf{U}}^\star)$ can be found by substituting (37) in (36). Once again, if $q_{\mathsf{U},0}^\star$ does not lie between 0 and 1, then the QoS constraint needs to be further relaxed by lowering ϵ_{U}.

Theorem 6. *Assuming that the point processes Φ and $\tilde{\Phi}$ are the same, an approximate lower bound of the success probability when we operate using LOAP is given by*

$$\mathbb{P}_{\mathrm{m,o1}}(\mathsf{U}) \geq \frac{(1-q_{\mathsf{U}})\lambda_{\mathrm{f}}}{\kappa^2\lambda_{\mathrm{m}} + (1-q_{\mathsf{U}})\lambda_{\mathrm{f}} + C(\alpha)\big\{\mu_{\mathrm{m}}\big(\frac{Q_{\mathrm{m}}\eta_{\mathrm{f}}}{Q_{\mathrm{f}}}\big)^{2/\alpha} + q_{\mathsf{U}}\lambda_{\mathrm{f}}\big(\frac{P_{\mathrm{f}}\eta_{\mathrm{f}}}{Q_{\mathrm{m}}}\big)^{2/\alpha} + (1-q_{\mathsf{U}})\lambda_{\mathrm{f}}\big(\frac{\eta_{\mathrm{f}}Q_{\mathrm{f}}}{Q_{\mathrm{m}}}\big)^{2/\alpha}\big\}} + \frac{\kappa^2\lambda_{\mathrm{m}}}{\kappa^2\lambda_{\mathrm{m}} + (1-q_{\mathsf{U}})\lambda_{\mathrm{f}} + C(\alpha)\{\mu_{\mathrm{m}}\eta_{\mathrm{m}}^{2/\alpha} + q_{\mathsf{U}}\lambda_{\mathrm{f}}(P_{\mathrm{f}}\eta_{\mathrm{m}}/Q_{\mathrm{m}})^{2/\alpha} + (1-q_{\mathsf{U}})\lambda_{\mathrm{f}}\eta_{\mathrm{m}}^{2/\alpha}\}}, \tag{30}$$

and in the case we operate using DOAP, an approximate lower bound of the success probability may be given by

$$\mathbb{P}_{\mathrm{m,o2}}(\mathsf{U}) \geq \frac{\lambda_{\mathrm{m}}\exp(-\pi R_{HO}^2(1-q_{\mathsf{U}})\lambda_{\mathrm{f}})}{\lambda_{\mathrm{m}} + \{(1-q_{\mathsf{U}})\lambda_{\mathrm{f}}\eta_{\mathrm{m}}^{2/\alpha} + \mu_{\mathrm{m}}\eta_{\mathrm{m}}^{2/\alpha} + q_{\mathsf{U}}\lambda_{\mathrm{f}}(P_{\mathrm{f}}\eta_{\mathrm{m}}/Q_{\mathrm{f}})^{2/\alpha}\}C(\alpha)} + \frac{(1-q_{\mathsf{U}})\lambda_{\mathrm{f}}(1-\exp(-\pi R_{HO}^2(A_{DOAP})))}{A_{DOAP}}. \tag{31}$$

where $A_{DOAP} = (1-q_{\mathsf{U}})\lambda_{\mathrm{f}} + C(\alpha)\{(1-q_{\mathsf{U}})\lambda_{\mathrm{f}}\eta_{\mathrm{f}}^{2/\alpha} + (\mu_{\mathrm{m}}Q_{\mathrm{m}}^{2/\alpha} + q_{\mathsf{U}}\lambda_{\mathrm{f}}P_{\mathrm{f}}^{2/\alpha})(\eta_{\mathrm{f}}/Q_{\mathrm{f}})^{2/\alpha}\}$.

Proof: The exact expressions for the success probabilities when the macro tier is in uplink is difficult to obtain. The first difficulty is due to the correlation between the point processes Φ and $\tilde{\Phi}$. To overcome this difficulty, we assume that R_{f} is small compared to the distances between MBSs. Consequently, we may assume the point processes Φ and $\tilde{\Phi}$ to be the same. The second difficulty is that, conditioned on the event the user connects to the Macro- (and respectively Femto-) tier, there is an exclusion zone surrounding the user where there aren't any other MBSs. However, it is difficult to take into account this exclusion region and hence we shall ignore the presence of this region. As such, the expressions we act as a lower bound of the actual success probability. □

Parameter	Value
α	4
λ_{m}	$8\times10^{-6}\mathrm{m}^{-2}$
μ_{m}	$20\lambda_{\mathrm{m}} = 1.6\times10^{-4}\mathrm{m}^{-2}$
$P_{\mathrm{m}}, Q_{\mathrm{m}}$	48 dBm, 20 dBm
$P_{\mathrm{f}}, Q_{\mathrm{f}}$	15 dBm, 10 dBm
$\gamma_{\mathrm{m}}, \eta_{\mathrm{m}}$	0 dB, 0 dB
$\gamma_{\mathrm{f}}, \eta_{\mathrm{f}}$	0 dB, 0 dB

TABLE I
PARAMETER VALUES USED IN NUMERICAL SECTION.

V. NUMERICAL RESULTS

In the following, we use the default values in Table I unless otherwise stated. We consider two cases where $\lambda_{\mathrm{f}} = \lambda_{\mathrm{m}}$ (sparse network) and $\lambda_{\mathrm{f}} = 100\lambda_{\mathrm{m}}$ (dense network). In addition, we consider the coverage distance of each FAP to be $R_{\mathrm{f}} = 10$m and 15m to demonstrate the role that coverage distance plays in our proposed CHDD scheme. Figures 4 and 5 plot the success probabilities of macrocell and femtocell transmission under CHDD scheme with varying q for macro tier in D and U mode, respectively. In these figures, we observe that femtocell success probabilities are generally much higher than the macrocell success probabilities because the FAP coverage distance R_{f} is small and fixed while the sparsity of MBSs makes the average macrocell transmission distance large. From Fig. 4, we observe that the optimal $q^\star$ that maximizes the respective success probability for macro and femto tiers is in complete agreement with our analysis given in remark 1. For the parameters considered, the macro tier has $q^\star = 0$ and femto tier $q^\star = 1$. In addition, we can see that the density of FAP has a significant effect on the success probabilities for both tiers. When the deployment of FAPs is significantly denser than that of MBSs, the CHDD scheme can only provide some improvement by optimally selecting q, implying that techniques such as interference avoidance, interference cancellation or access control are required to provide better performance. On the other hand, we see that the proposed CHDD scheme can bring about a significant improvement in success probability to the femto tier when the deployment of FAPs is sparse by allowing cognitive femtocells to operate in $q^\star = 1$ (uplink transmissions). Furthermore, by decreasing R_{f}, the success probability of femto tier can be improved quite drastically showing the importance of controlling the coverage distance for interference management. For the uplink mode in Fig. 5, our analysis in remark 2 also matches the numerical results. In addition, the effect of FAP density and R_{f} on the success probabilities is similar to the D case discussed above. Note that the macro tier success probability in uplink mode is significantly small due to the absence of power control and large macrocell transmission distance. However, it will be apparent that this can be significantly improved by introducing open access FAPs.

Fig. 6 plots the success probability of the femto tier when the macro tier is in downlink and for a very dense deployment of FAPs, which could happen in buildings or housing apartments. From these plots, we see that the success probability can sometimes attain a maxima or a minima in $(0,1)$. The existence of a interior minima can be used to further demonstrate the importance of choosing q: FAPs can gain a higher overall throughput by agreeing to be in downlink in the in the same time slots (and respectively uplink) instead choosing independently (which corresponds to the case of an intermediate q). This can be achieved by the proposed framework of having the macro-tier to broadcast control signals.

Next, we show how cognitive FAPs operating with our

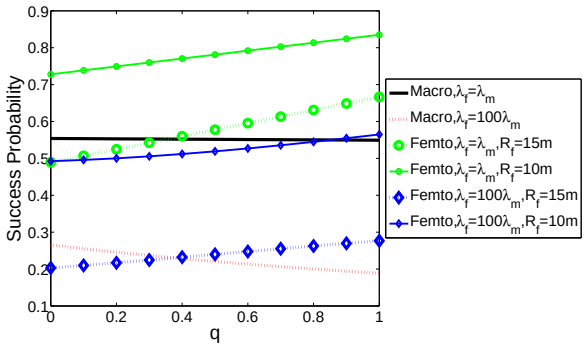

Fig. 4. Success probability when macro tier is in downlink mode.

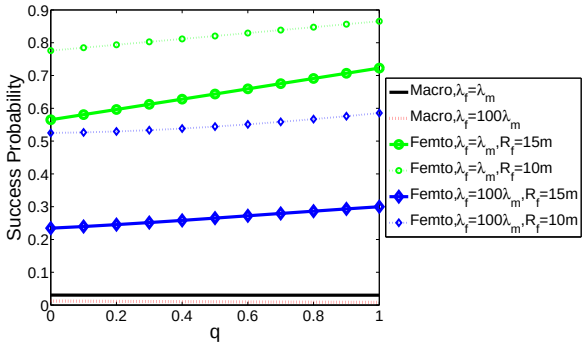

Fig. 5. Success probability when macro tier is in uplink mode.

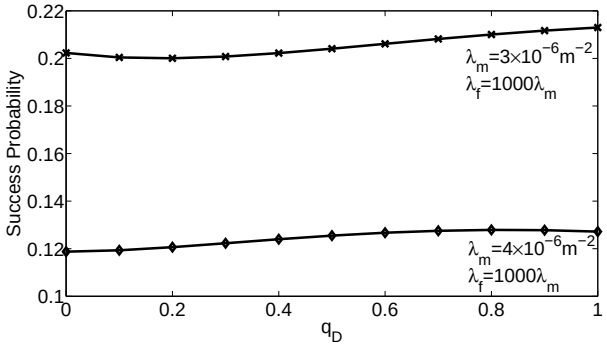

Fig. 6. Femto success probability with Macro in downlink, very dense Femto tier deployment, $R_{\mathrm{f}} = 10$m.

proposed open access policy (OAP) can improve the macro tier success probability significantly. We start by discussing the *distance based OAP*. Figures 7 and 8 show the success probabilities of macrocell transmission under CHDD scheme with varying $\lambda_{\mathrm{f}}/\lambda_{\mathrm{m}}$ for macro tier in D and U mode, respectively. By comparing with CHDD scheme operating with a closed access policy, we see that the OAP always improves the success probability of a transmission, with the exception of the macro tier in downlink case with $\mathrm{R_{HO}} = 40$m. From both graphs, we see that operating OAP offers a significant improvement when there is a high probability of finding a femtocell operating in the same mode as the macro tier. On the other hand, the OAP offers a significantly smaller improvement if the majority of the femtocells does not operate in the same mode as the macro tier. We also observe that for macro tier in downlink, the success probability when $q = 0.9$ drops initially with increasing $\lambda_{\mathrm{f}}/\lambda_{\mathrm{m}}$ before increasing. This can be explained by that mobile users experience the effects of added interference before a critical density of FAPs is reached, and after which, mobile users experience the benefit of having a nearby FAPs to connect to. This tells us the OAP is most useful in a dense setting. For the same set of curves, we also see that $\mathrm{R_{HO}} = 10$m offers the best coverage over most values of $\lambda_{\mathrm{f}}/\lambda_{\mathrm{m}}$, and importantly, is an improvement over the closed access policy. This is as opposed to $\mathrm{R_{HO}} = 40$m, which initially experiences poorer coverage. This can be explained by that, when $\mathrm{R_{HO}}$ is too large, mobile users may be forced to hand over to an FAP which offers poorer coverage than the nearest MBS. In the case where $\mathrm{R_{HO}} = 10$m, while it remains an improvement over the closed access policy, it requires a higher density before the effects of the OAP may be felt. We can explain this by that increasing $\mathrm{R_{HO}}$ also increases the probability that a mobile user falls within the range of a FAP. The same comments can be made for the macro tier in uplink case. In summary, these two plots suggest that, in order for this policy to work well, $\mathrm{R_{HO}}$ has to trade off being large enough so that many FAPs will be in range, while ensuring that the FAP users it serves enjoy a better success probability than if they connected to the MBS.

Figure 9 and Figure 10 shows the cognitive FAPs operating with both sets of OAPs in the cases where the macro tier is in downlink and uplink, respectively. There does not appear to be a common κ^{D} (respectively, κ^{U}) that is optimal for all values of q^{D} (respectively, q^{U}) simultaneously. We chose $\kappa^{\mathsf{D}} = (P_{\mathrm{f}}/P_{\mathrm{m}})^{1/\alpha}$ and $\kappa^{\mathsf{U}} = 1$ as it appears to be a good compromise. From the plots, we observe that the LOAP always performs better than the DOAP. In Figure 9, we observe that the LOAP performs at approximately the same performance for $\lambda_{\mathrm{f}}/\lambda_{\mathrm{m}}$ up to 100, for various values of q, before the policy begins to suffer due to the overwhelming density of interferers. The DOAP, however, appears to suffer from the increased density of interferers for a much smaller value of $\lambda_{\mathrm{f}}/\lambda_{\mathrm{m}}$. Figure 10 shows a general increase in success probabilities in all cases. From both plots, we can observe that, taking $\lambda_{\mathrm{f}}/\lambda_{\mathrm{m}} = 100$ for example, the additional knowledge of the location of the MBS can double the success probability. In conclusion, by looking at the previous four plots on the open access policy, we observe that while it is generally difficult to ascertain a single criterion that is optimal for both uplink, downlink, and all values of q_{U} and q_{D} simultaneously, operating an open acccess policy is generally beneficial to macrocell users. Figure 11 shows the total network throughput with respect to q for macro tier in D and U modes, respectively. In this figure, R_{f} is set as 15m and we consider both sparse and dense FAP deployment. For sparse FAP deployment, it can be seen that the total network throughput remains almost constant with respect to q, regardless of whether the macro tier is in D or U mode. Although we see that by choosing $q^{\star} = 1$ in Figs. 4 and 5, there is a significant improvement in success probability to the femto tier for sparse network. However, we do not see this effect in Fig. 11 since the number

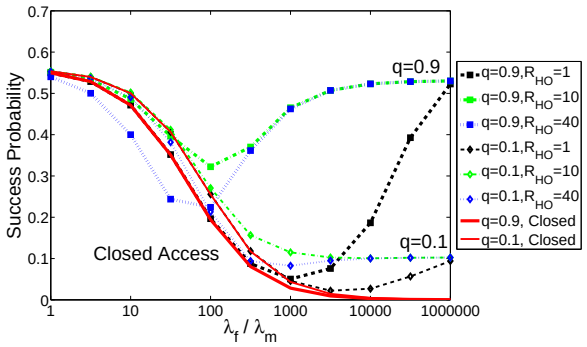

Fig. 7. Macro success probability with the distance-based open access policy, when macro tier is in downlink mode.

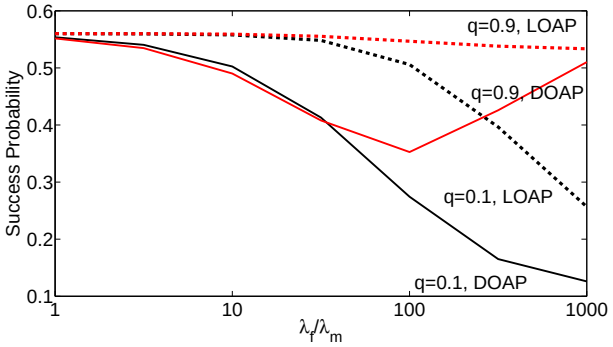

Fig. 9. Macro success probability with macro tier in D and location-based open access policy, with $\kappa_{\mathrm{D}} = (P_{\mathrm{f}}/P_{\mathrm{m}})^{1/4}$ and $\mathrm{R_{HO}} = 10$m.

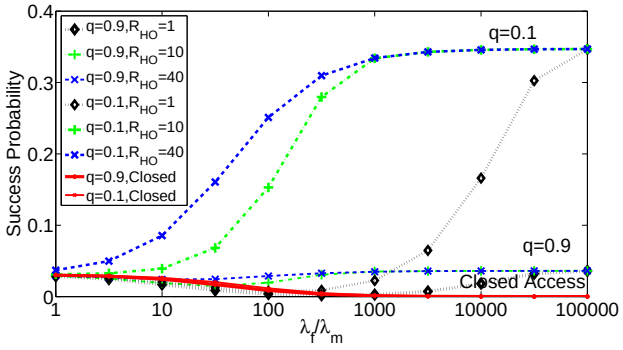

Fig. 8. Lower Bound of Macro success probability with the distance-based open access policy, when macro tier is in uplink mode.

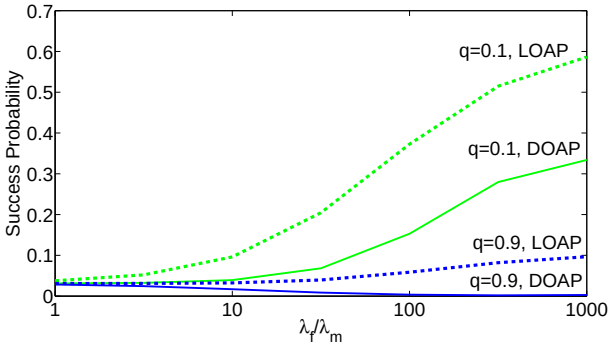

Fig. 10. Lower Bound of Macro success probability with macro tier in U and location-based open access policy, with $\kappa_{\mathrm{D}} = 1$ and $\mathrm{R_{HO}} = 10$m.

of femtocells is too small to create a substantial improvement in the total network throughout. On the other hand, we clearly see that $q^\star = 1$ is optimal in maximizing the total network throughput for dense network. The main reason is that the throughput associated with the femto tier essentially dominates the total network throughput and thus the CHDD scheme can bring about a throughput improvement by selecting $q^\star = 1$. In addition, Fig. 11 also support our previous analysis that the maximum total network throughput is attained at either $q = 0$ or $q = 1$.

VI. Conclusion and Discussion

In this work, we proposed a CHDD scheme in which FDD is performed on the macrocell and TDD is simultaneously operated in these bands by the underlaid cognitive femtocells. Using tools from stochastic geometry, we provided a spatial randomness-aware methodology on how to design optimal switching mechanism for cognitive TDD operation of femtocells. We derived performance measures in terms of success probability, total throughput, and spatial average capacity for our proposal CHDD scheme for macro tier in downlink and uplink mode, respectively. We proposed an open access policy and investigated the effect of combining open access FAPs with CHDD scheme in terms of macrocell transmit success probability. Numerical results showed the effectiveness of our proposed CHDD scheme for improving the overall network performance and provided practical relevant guidelines on how to optimally choose the uplink-downlink mode multiplexing probability of the femto tier. Furthermore, we showed that open access policies are effective for interference management, especially in dense deployment. Overall, this work provides essential understanding for successful deployment of future cognitive femtocell networks.

Appendix

A. Preliminaries

As it is extensively used in the proofs and to avoid repetition, using the Laplace transform of the aggregate interference, we provide first the success probability for a transmitter and receiver pair, at distance r apart, where the transmitter transmits at P and interferers transmit at Q, i.e.

$$\begin{aligned}&\mathbb{P}(\mathsf{SIR} > \gamma)\\ &\overset{(a)}{=} \mathbb{P}\left(\frac{Phr^{-\alpha}}{\sum_{x\in\Theta_0} Qh_x x^{-\alpha}} > \gamma\right)\\ &\overset{(b)}{=} \mathbb{E}_{\Theta_0,h_x}\left[\exp\left(-\frac{\gamma r^\alpha}{P}\left(\sum_{x\in\Theta_0} Qh_x x^{-\alpha}\right)\right)\right], \end{aligned} \quad (38)$$

where h, h_x are independent $\exp(1)$ random variables, (a) follows by definition, and (b) by taking expectation over h. If Θ_0 is distributed according to a homogeneous PPP λ conditioned on that the nearest interferer is at least s away,

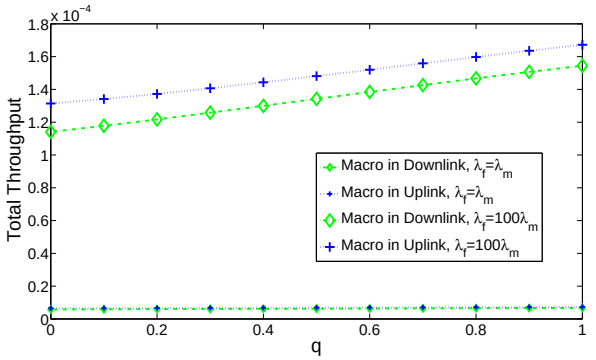

Fig. 11. Total network throughput.

then the Laplace transform is given by

$$\begin{aligned}&\mathbb{E}_{\Theta_0,h_x}\left[\exp\left(-\frac{\gamma r^\alpha}{P}\left(\sum_{x\in\Theta_0} Qh_x x^{-\alpha}\right)\right)\right]\\ &\overset{(c)}{=}\exp\left(-2\pi\lambda\int_{z=s}^{\infty}\left(1-\mathbb{E}_{h_z}\left(\frac{\gamma r^\alpha Q h_z}{Pz^\alpha}\right)\right)z\mathrm{d}z\right)\\ &=\exp\left(-2\pi\lambda\int_{z=s}^{\infty}\left(1-\frac{1}{1+\gamma r^\alpha Q/Pz^\alpha}\right)z\mathrm{d}z\right)\end{aligned}\quad(39)$$

where (c) follows from a result involving PPPs. Detailed computations and explanations may be found in [7], [25]. When $s=0$, the expression simplifies to $\exp(-\pi r^2\lambda C(\alpha)(Q\gamma/P)^{2/\alpha})$, and when $s=r$, the expression simplifies to $\exp(-\pi r^2\lambda(Q/P)^{2/\alpha}\rho(\gamma,\alpha))$.

B. Proof of Theorem 1

We first begin by deriving (4) as follows:

$$\begin{aligned}&\mathbb{P}_{\mathrm{m}}(\mathsf{D})\\ &=\int_0^\infty \mathbb{E}_{\Theta,\Phi,\tilde{\Phi}}\left[\exp\left(-\frac{\gamma_{\mathrm{m}} r^\alpha}{P_{\mathrm{m}}}\left(\sum_{x\in\Theta\setminus x_0} P_{\mathrm{m}}h_x x^{-\alpha}\right.\right.\right.\\ &\qquad\left.\left.\left.+\sum_{y\in\Phi} P_{\mathrm{f}}h_y y^{-\alpha}+\sum_{z\in\tilde{\Phi}} Q_{\mathrm{f}}h_z z^{-\alpha}\right)\right)\right]f(r)\mathrm{d}r\\ &\overset{(a)}{=}\int_0^\infty \mathbb{E}_\Theta\left[\exp\left(-\gamma_{\mathrm{m}}r^\alpha\left(\sum_{x\in\Theta\setminus x_0}(P_{\mathrm{m}}/P_{\mathrm{m}})h_x x^{-\alpha}\right)\right)\right]\\ &\quad\mathbb{E}_{\Phi^{\mathsf{D}}}\left[\exp\left(-\gamma_{\mathrm{m}}r^\alpha\left(\sum_{y\in\Phi^{\mathsf{D}}}(P_{\mathrm{f}}/P_{\mathrm{m}})h_y y^{-\alpha}\right)\right)\right]\\ &\quad\mathbb{E}_{\Phi^{\mathsf{U}}}\left[\exp\left(-\gamma_{\mathrm{m}}r^\alpha\left(\sum_{z\in\Phi^{\mathsf{U}}}(Q_{\mathrm{f}}/P_{\mathrm{m}})h_z z^{-\alpha}\right)\right)\right]f(r)\mathrm{d}r\\ &\overset{(b)}{=}\int_0^\infty \exp\left(-\pi r^2\lambda_{\mathrm{m}}\rho(\gamma_{\mathrm{m}},\alpha)\right)\exp\left(-\pi r^2\left(q_{\mathsf{D}}\lambda_{\mathrm{f}}P_{\mathrm{f}}^{2/\alpha}\right.\right.\\ &\qquad\left.\left.+(1-q_{\mathsf{D}})\lambda_{\mathrm{f}}Q_{\mathrm{f}}^{2/\alpha}\right)C(\alpha)(\gamma_{\mathrm{m}}/P_{\mathrm{m}})^{2/\alpha}\right)f(r)\mathrm{d}r\\ &\overset{(c)}{=}\frac{\lambda_{\mathrm{m}}}{\lambda_{\mathrm{m}}+\lambda_{\mathrm{m}}\rho(\gamma_{\mathrm{m}},\alpha)+\lambda_{\mathrm{f}}D(q)C(\alpha)(\gamma_{\mathrm{m}}/P_{\mathrm{m}})^{2/\alpha}}\end{aligned}$$

where (a) by the independence of the PPPs; (b) by the Slivnyak's Theorem and the Laplace transforms of the macro and femto tier interference terms; and (c) integrating with respect to the pdf $f(r)=2\pi\lambda_{\mathrm{m}}r\exp(-\lambda_{\mathrm{m}}\pi r^2)$ to obtain the desired result. Next, we continue with deriving (5) as follows:

$$\begin{aligned}&\mathbb{P}_{\mathrm{f},\mathsf{D}}(\leftrightarrow)\\ &\overset{(a)}{=}q_{\mathsf{D}}\mathbb{P}_{\mathrm{f},\mathsf{D}}(\rightarrow)+(1-q_{\mathsf{D}})\mathbb{P}_{\mathrm{f},\mathsf{D}}(\leftarrow)\\ &\overset{(b)}{=}q_{\mathsf{D}}\mathbb{E}_{\Theta,\Phi,\tilde{\Phi}}\left[\exp\left(-\frac{\gamma_{\mathrm{f}}r^\alpha}{P_{\mathrm{f}}}\left(\sum_{x\in\Theta}P_{\mathrm{m}}h_x x^{-\alpha}\right.\right.\right.\\ &\qquad\left.\left.\left.+\sum_{y\in\Phi^{\mathsf{D}}\setminus 0}P_{\mathrm{f}}h_y y^{-\alpha}+\sum_{z\in\tilde{\Phi}^{\mathsf{U}}}Q_{\mathrm{f}}h_z z^{-\alpha}\right)\right)\right]\\ &\quad+(1-q_{\mathsf{D}})\mathbb{E}_{\Theta,\Phi,\tilde{\Phi}}\left[\exp\left(-\frac{\eta_{\mathrm{f}}r^\alpha}{Q_{\mathrm{f}}}\left(\sum_{x\in\Theta}P_{\mathrm{m}}h_x x^{-\alpha}\right.\right.\right.\\ &\qquad\left.\left.\left.+\sum_{y\in\Phi^{\mathsf{D}}\setminus 0}P_{\mathrm{f}}h_y y^{-\alpha}+\sum_{z\in\tilde{\Phi}^{\mathsf{U}}}Q_{\mathrm{f}}h_z z^{-\alpha}\right)\right)\right]\\ &\overset{(c)}{=}q_{\mathsf{D}}\mathbb{E}_\Theta\left[\exp\left(-\gamma_{\mathrm{f}}r^\alpha\left(\sum_{x\in\Theta}(P_{\mathrm{m}}/P_{\mathrm{f}})h_x x^{-\alpha}\right)\right)\right]\\ &\quad\mathbb{E}_\Phi\left[\exp\left(-\gamma_{\mathrm{f}}r^\alpha\left(\sum_{y\in\Phi^{\mathsf{D}}\setminus 0}(P_{\mathrm{f}}/P_{\mathrm{f}})h_y y^{-\alpha}\right)\right)\right]\\ &\quad\mathbb{E}_{\tilde{\Phi}}\left[\exp\left(-\gamma_{\mathrm{f}}r^\alpha\left(\sum_{z\in\tilde{\Phi}^{\mathsf{U}}}(Q_{\mathrm{f}}/P_{\mathrm{f}})h_z z^{-\alpha}\right)\right)\right]\\ &\quad+(1-q_{\mathsf{D}})\mathbb{E}_\Theta\left[\exp\left(-\eta_{\mathrm{f}}r^\alpha\left(\sum_{x\in\Theta}(P_{\mathrm{m}}/Q_{\mathrm{f}})h_x x^{-\alpha}\right)\right)\right]\\ &\quad\mathbb{E}_\Phi\left[\exp\left(-\eta_{\mathrm{f}}r^\alpha\left(\sum_{y\in\Phi^{\mathsf{D}}\setminus 0}(P_{\mathrm{f}}/Q_{\mathrm{f}})h_y y^{-\alpha}\right)\right)\right]\\ &\quad\mathbb{E}_{\tilde{\Phi}}\left[\exp\left(-\eta_{\mathrm{f}}r^\alpha\left(\sum_{z\in\tilde{\Phi}^{\mathsf{U}}}(Q_{\mathrm{f}}/Q_{\mathrm{f}})h_z z^{-\alpha}\right)\right)\right]\\ &\overset{(d)}{=}q_{\mathsf{D}}\exp\left(-\pi\frac{R_{\mathrm{f}}^2}{P_{\mathrm{f}}^{2/\alpha}}\left(\lambda_{\mathrm{m}}P_{\mathrm{m}}^{2/\alpha}+q_{\mathsf{D}}\lambda_{\mathrm{f}}P_{\mathrm{f}}^{2/\alpha}\right.\right.\\ &\qquad\left.\left.+(1-q_{\mathsf{D}})\lambda_{\mathrm{f}}Q_{\mathrm{f}}^{2/\alpha}\right)C(\alpha)\gamma_{\mathrm{f}}^{2/\alpha}\right)\\ &\quad+(1-q_{\mathsf{D}})\exp\left(-\pi\frac{R_{\mathrm{f}}^2}{Q_{\mathrm{f}}^{2/\alpha}}\left(\lambda_{\mathrm{m}}P_{\mathrm{m}}^{2/\alpha}+q_{\mathsf{D}}\lambda_{\mathrm{f}}P_{\mathrm{f}}^{2/\alpha}\right.\right.\\ &\qquad\left.\left.+(1-q_{\mathsf{D}})\lambda_{\mathrm{f}}Q_{\mathrm{f}}^{2/\alpha}\right)C(\alpha)\eta_{\mathrm{f}}^{2/\alpha}\right)\end{aligned}$$

where in (a) we condition on that the typical FAP is in downlink or in uplink mode; (b) the Laplace Transform is simply equivalent to the probability of a successful transmission; (c) by the independence of the PPPs and Slivnyak's Theorem; and (d) by the Laplace transforms of the macro and femto tier interference terms. Note that unlike the derivation of (4), we do not need to take the expectation over r because the distance between the femtocell user and the FAP is fixed at R_{f}.

C. Proof of argument that $q_{\mathsf{D}}^\star\in\{0,1\}$

There are two possibilities, either the maxima occurs as an interior point $(0,1)$ (which has to be found numerically), or the maxima occurs as one of $\{0,1\}$. We can determine which case it is by looking at the first order condition. By the first

order condition, any turning point q_{D} satisfies

$$\frac{1+(1-q_{\mathsf{D}})(\pi R_{\mathrm{f}}^2 C(\alpha)(\eta_{\mathrm{f}}/Q_{\mathrm{f}})^{2/\alpha}\lambda_{\mathrm{f}}(P_{\mathrm{f}}^{2/\alpha}-Q_{\mathrm{f}}^{2/\alpha}))}{1-q_{\mathsf{D}}\pi R_{\mathrm{f}}^2 C(\alpha)(\gamma_{\mathrm{f}}/P_{\mathrm{f}})^{2/\alpha}\lambda_{\mathrm{f}}(P_{\mathrm{f}}^{2/\alpha}-Q_{\mathrm{f}}^{2/\alpha})} = \exp\Bigg(\pi R_{\mathrm{f}}^2\big(\lambda_{\mathrm{m}}P_{\mathrm{m}}^{2/\alpha}+\lambda_{\mathrm{f}}Q_{\mathrm{f}}^{2/\alpha}+q_{\mathsf{D}}\lambda_{\mathrm{f}}(P_{\mathrm{f}}^{2/\alpha}-Q_{\mathrm{f}}^{2/\alpha})\big) C(\alpha)\big(\big(\frac{\eta_{\mathrm{f}}}{Q_{\mathrm{f}}}\big)^{2/\alpha}-\big(\frac{\gamma_{\mathrm{f}}}{P_{\mathrm{f}}}\big)^{2/\alpha}\big)\Bigg) \quad (40)$$

The next step is essentially a curve sketching argument. Write the equation in the form $\frac{1+a(1-x)}{1-bx}=\exp(cx+d)$. By the assumption $P_{\mathrm{f}}\eta_{\mathrm{f}} > Q_{\mathrm{f}}\gamma_{\mathrm{f}}$, we have $a,b,c,d>0$. The LHS has an asymptote at $x=1/b$. Substitute $x=1/b$ into the numerator. There are essentially 3 types of curves, determined by the following cases: $\{b<\frac{a}{1+a}, b=\frac{a}{1+a}, b>\frac{a}{1+a}\}$.

1) $b<\frac{a}{1+a}$: By looking at the right of the asymptote, if $1/b \geq 1$ then the right side has no turning points in $[0,1]$. This is trivially satisfied by the original condition $b<\frac{a}{1+a}$. By looking the the left side, we see that there is a turning point in $[0,1]$ iff $\exp(d)\leq 1+a$.
2) $b>\frac{a}{1+a}$: This is the trickiest to analyze and hence we shall leave this case to a numerical computation.
3) $b=\frac{a}{1+a}$: The LHS expression $\frac{1+a(1-x)}{1-bx}$ simplifies to $1+a$. To check if there is a turning point in $[0,1]$, let $x=1$. There is an interior maxima in $(0,1)$ if $\exp(c+d)>a+1$, none otherwise.

Of the above, only the case $b<\frac{a}{1+a}$ gives us an easy characterization of a case where the function has no turning points in $[0,1]$, following which we can conclude that the maxima must be in $\{0,1\}$. However, the conclusion that the maxima is one of $\{0,1\}$ is also valid if the turning point is a minima. The occurence of this case is demonstrated in the numerical results section.

D. Proof of Theorem 2 and Theorem 5

The spatial average capacity is given by $\mathbb{E}[\log(1+\mathsf{SIR})]$ and this is equal to $\int_{t=0}^{\infty}\mathbb{P}(\mathsf{SIR}>e^t-1)\mathrm{d}t$ [25]. The expressions for the general case follow from this definition.

Next, note that by the substitution $z=\sqrt{e^t-1}$, we have $\int_{t=0}^{\infty} f(e^t-1)\mathrm{d}t = \int_{z=0}^{\infty} f(z)\frac{2z}{z^2+1}\mathrm{d}z$. Consider next the macrocell downlink case. The macrocell spatial average capacity is straightforward from the above definitions. We derive the femtocell spatial average capacity as follows:

$$\begin{aligned} R_{\mathrm{f,D}}(\leftrightarrow) &= \mathbb{E}[\log(1+\mathsf{SIR})] \\ &\overset{(a)}{=} q_{\mathsf{D}}\int_0^{\infty}\frac{2x\exp(-A_1x)}{x^2+1}\mathrm{d}x \\ &+ (1-q_{\mathsf{D}})\int_0^{\infty}\frac{2x\exp(-A_2x)}{x^2+1}\mathrm{d}x \\ &\overset{(b)}{=} q_{\mathsf{D}}(\sin A_1(\pi-2\mathrm{Si}(A_1))-2\mathrm{Ci}(A_1)\cos A_1) \\ &+ (1-q_{\mathsf{D}})(\sin A_2(\pi-2\mathrm{Si}(A_2))-2\mathrm{Ci}(A_2)\cos A_2) \end{aligned}$$

where (a) follows substituting (5) with $\alpha=4$, $\gamma_{\mathrm{f}}=\eta_{\mathrm{f}}=e^t-1$, and using the above simplifications; (b) follows from integrating the indefinite integral.

Suppose now that we consider the macrocell uplink case, and we use the simplified notation $B_{\mathsf{U}}=\big(\mu_{\mathrm{m}}+q_{\mathsf{U}}\lambda_{\mathrm{f}}\sqrt{\frac{P_{\mathrm{f}}}{Q_{\mathrm{m}}}}+(1-q_{\mathsf{U}})\lambda_{\mathrm{f}}\sqrt{\frac{Q_{\mathrm{f}}}{Q_{\mathrm{m}}}}\big)\pi/2$. The macrocell spatial average capacity is then given by

$$\begin{aligned} R_{\mathrm{m}}(\mathsf{U}) &= \mathbb{E}[\log(1+\mathsf{SIR})] \overset{(a)}{=} \int_0^{\infty}\frac{1}{\lambda_{\mathrm{m}}+B_{\mathsf{U}}(e^t-1)^{1/2}}\mathrm{d}t \\ &\overset{(b)}{=} \frac{2\lambda_{\mathrm{m}}\log(\lambda_{\mathrm{m}}/B_{\mathsf{U}})+B_{\mathsf{U}}\pi}{\lambda_{\mathrm{m}}^2+B_{\mathsf{U}}^2} \end{aligned}$$

where (a) follows from substituting $\alpha=4$ into (19), $\eta_{\mathrm{m}}=e^t-1$, and using the above simplifications; (b) from evaluating the indefinite integral. The derivation of the femtocell spatial average capacity in the uplink case is almost identical to the downlink case.

E. Proof of Theorem 3

The success probability when we operate the MBS and FAP location-based policy is given by (41) where $\mathbb{E}_{\Theta}[\exp(-(\gamma_{\mathrm{m}}r^{\alpha}/P_{\mathrm{m}})(\sum_{\Theta\setminus x_0}P_m h_x x^{-\alpha}))|\mathrm{M}] = \exp(-\pi r^2\lambda_{\mathrm{m}}\rho(\gamma_{\mathrm{m}},\alpha))$ and $\mathbb{E}_{\Phi}[\exp(-(\gamma_{\mathrm{m}}r^{\alpha}/P_{\mathrm{m}})(\sum_{\Phi^{\mathsf{D}}\setminus y_0}P_{\mathrm{f}}h_y y^{-\alpha}))|\mathrm{M}] = \exp(-\pi r^2\kappa^2 q_{\mathsf{D}}\lambda_{\mathrm{f}}\rho(\gamma_{\mathrm{m}}P_{\mathrm{f}}/\kappa^{\alpha}P_{\mathrm{m}},\alpha))$ are the Laplace transform of the interference due to the macro tier and the femto tier in downlink, respectively, conditioned on the event that $\kappa r < s$ where r,s are the distances to the nearest MBS and nearest FAP, respectively, $\mathbb{E}_{\tilde{\Phi}}[\exp(-(\gamma_{\mathrm{m}}r^{\alpha}/P_{\mathrm{m}})(\sum_{\tilde{\Phi}^{\mathsf{U}}}Q_{\mathrm{f}}h_z z^{-\alpha}))|\mathrm{M}] = \exp(-\pi r^2\lambda_{\mathrm{f}}(1-q_{\mathsf{D}})(Q_{\mathrm{f}}\gamma_{\mathrm{m}}/P_{\mathrm{m}})^{2/\alpha}C(\alpha))$ is the Laplace transform of the interference due to the femto tier in uplink, unconditioned, and $f_{\mathrm{m|M}}(r) = 2\pi r(\lambda_{\mathrm{m}}+q_{\mathsf{D}}\lambda_{\mathrm{f}}\kappa^2)\exp(-\pi r^2(\lambda_{\mathrm{m}}+q_{\mathsf{D}}\lambda_{\mathrm{f}}\kappa^2))$ is the pdf of the nearest MBS conditioned on that the user connects to the macro tier (equivalently, $\kappa r < s$). The terms $\mathbb{E}_{\Theta}[\ldots|\mathrm{F}] = \exp(-\pi(r/\kappa)^2\lambda_{\mathrm{m}}\rho(\gamma_{\mathrm{f}}P_{\mathrm{m}}\kappa^{\alpha}/P_{\mathrm{f}},\alpha))$, $\mathbb{E}_{\Phi}[\ldots|\mathrm{F}] = \exp(-\pi r^2 q_{\mathsf{D}}\lambda_{\mathrm{f}}\rho(\gamma_{\mathrm{f}},\alpha))$ and $\mathbb{E}_{\tilde{\Phi}}[\ldots|\mathrm{F}] = \exp(-\pi r^2(1-q_{\mathsf{D}})\lambda_{\mathrm{f}}(Q_{\mathrm{f}}\gamma_{\mathrm{f}}/P_{\mathrm{f}})^{2/\alpha}C(\alpha))$ are also Laplace transforms of the interference similarly defined previously, except that the Laplace transforms are conditioned on the event that the user connects to the femto tier (equivalently, $\kappa r > s$). Similarly, $f_{\mathrm{f|F}}(r) = 2\pi r(\lambda_{\mathrm{m}}/\kappa^2+q_{\mathsf{D}}\lambda_{\mathrm{f}})\exp(-\pi r^2(\lambda_{\mathrm{m}}/\kappa^2+q_{\mathsf{D}}\lambda_{\mathrm{f}}))$ is the pdf of the nearest MBS conditioned on $\kappa r > s$.

We also have that (a) follows from conditioning on the event the user connects to the macro tier or the femto tier, and (b) is adapted from a similar calculation in [14].

We now compute the downlink success probability when we operate the distance-based open access policy: Let r be the distance to the nearest FAP operating in downlink mode. r is thus a r.v. with pdf $2\pi q_{\mathsf{D}}\lambda_{\mathrm{f}} r\exp(-\pi r^2 q_{\mathsf{D}}\lambda_{\mathrm{f}})$. By considering the event where the user is located within R_{HO} of a FAP, the success probability for this policy may be written as

$$\begin{aligned} \mathbb{P}_{\mathrm{m,o2}}(\mathsf{D}) = \mathbb{P}_{\mathrm{f}}(\mathsf{D}|r<\mathrm{R}_{\mathsf{HO}})\mathbb{P}(r<\mathrm{R}_{\mathsf{HO}}) \\ +\mathbb{P}_{\mathrm{m}}(\mathsf{D}|r\geq\mathrm{R}_{\mathsf{HO}})\mathbb{P}(r\geq\mathrm{R}_{\mathsf{HO}}) \quad (42) \end{aligned}$$

We start by computing the success probability due to the user connecting to the femto tier: (see (43)) where (a) conditions on the event that the nearest downlink FAP is at r, and (b) splits the success probability of a single transmission into the Laplace transforms of the interference due to the following: the

$$\begin{aligned}
\mathbb{P}_{\mathrm{m,o1}}(\mathsf{D}) &\overset{(a)}{=} \mathbb{P}_{\mathrm{m,o1}}(\mathsf{D}|\mathrm{M})\mathbb{P}(\mathrm{M}) + \mathbb{P}_{\mathrm{m,o1}}(\mathsf{D}|\mathrm{F})\mathbb{P}(\mathrm{F}) \\
&\overset{(b)}{=} \int_{r=0}^{\infty} \mathbb{E}_{\Theta}[\exp(-\frac{\gamma_{\mathrm{m}} r^{\alpha}}{P_{\mathrm{m}}}(\sum_{\Theta\setminus x_0} P_m h_x x^{-\alpha}))|\mathrm{M}]\mathbb{E}_{\Phi}[\exp(-\frac{\gamma_{\mathrm{m}} r^{\alpha}}{P_{\mathrm{m}}}(\sum_{\Phi^{\mathsf{D}}\setminus y_0} P_{\mathrm{f}} h_y y^{-\alpha}))|\mathrm{M}] \\
&\qquad \times \mathbb{E}_{\tilde{\Phi}}[\exp(-\frac{\gamma_{\mathrm{m}} r^{\alpha}}{P_{\mathrm{m}}}(\sum_{\tilde{\Phi}^{\mathsf{U}}} Q_{\mathrm{f}} h_z z^{-\alpha}))|\mathrm{M}] f_{\mathrm{m}|\mathrm{M}}(r)dr \frac{\lambda_{\mathrm{m}}}{\kappa^2 q_{\mathsf{D}}\lambda_{\mathrm{f}} + \lambda_{\mathrm{m}}} \\
&+ \int_{r=0}^{\infty} \mathbb{E}_{\Theta}[\exp(-\frac{\gamma_{\mathrm{m}} r^{\alpha}}{P_{\mathrm{f}}}(\sum_{\Theta} P_{\mathrm{m}} h_x x^{-\alpha}))|\mathrm{F}]\mathbb{E}_{\Phi}[\exp(-\frac{\gamma_{\mathrm{m}} r^{\alpha}}{P_{\mathrm{f}}}(\sum_{\Phi^{\mathsf{D}}} P_{\mathrm{f}} h_y y^{-\alpha}))|\mathrm{F}] \\
&\qquad \times \mathbb{E}_{\tilde{\Phi}}[\exp(-\frac{\gamma_{\mathrm{m}} r^{\alpha}}{P_{\mathrm{f}}}(\sum_{\tilde{\Phi}^{\mathsf{U}}} Q_{\mathrm{f}} h_z z^{-\alpha}))|\mathrm{F}] f_{\mathrm{f}|\mathrm{F}}(r)dr \frac{q_{\mathsf{D}}\lambda_{\mathrm{f}}}{q_{\mathsf{D}}\lambda_{\mathrm{f}} + \kappa^2\lambda_{\mathrm{m}}} \\
&= \lambda_{\mathrm{m}}/\{\lambda_{\mathrm{m}}(1+\rho(\gamma_{\mathrm{m}},\alpha)) + \kappa^2 q_{\mathsf{D}}\lambda_{\mathrm{f}}(1+\rho(\gamma_{\mathrm{m}}P_{\mathrm{f}}/\kappa^{\alpha}P_{\mathrm{m}},\alpha)) + (1-q_{\mathsf{D}})\lambda_{\mathrm{f}}(Q_{\mathrm{f}}\gamma_{\mathrm{m}}/P_{\mathrm{m}})^{2/\alpha}C(\alpha)\} \\
&+ q_{\mathsf{D}}\lambda_{\mathrm{f}}/\{(1/\kappa^2)\lambda_{\mathrm{m}}(1+\rho(\gamma_{\mathrm{f}}P_{\mathrm{m}}\kappa^{\alpha}/P_{\mathrm{f}},\alpha)) + q_{\mathsf{D}}\lambda_{\mathrm{f}}(1+\rho(\gamma_{\mathrm{f}},\alpha)) + (1-q_{\mathsf{D}})\lambda_{\mathrm{f}}(Q_{\mathrm{f}}\gamma_{\mathrm{f}}/P_{\mathrm{f}})^{2/\alpha}C(\alpha)\} \qquad (41)
\end{aligned}$$

$$\begin{aligned}
&\mathbb{P}_{\mathrm{f}}(\mathsf{D}|r < \mathrm{R}_{\mathsf{HO}})\mathbb{P}(r < \mathrm{R}_{\mathsf{HO}}) \\
&\overset{(a)}{=} \int_{r=0}^{\mathrm{R}_{\mathsf{HO}}} \mathbb{P}(\mathsf{D}|r) f_{\mathrm{f}}(r)dr \overset{(b)}{=} \int_{r=0}^{\mathrm{R}_{\mathsf{HO}}} \exp(-\pi r^2 q_{\mathsf{D}}\lambda_{\mathrm{f}}\rho(\gamma_{\mathrm{f}},\alpha)) \exp(-\pi r^2 \lambda_{\mathrm{m}}(P_{\mathrm{m}}\gamma_{\mathrm{f}}/P_{\mathrm{f}})^{2/\alpha}C(\alpha)) \\
&\exp(-\pi r^2(1-q_{\mathsf{D}})\lambda_{\mathrm{f}}(Q_{\mathrm{f}}\gamma_{\mathrm{f}}/P_{\mathrm{f}})^{2/\alpha}C(\alpha))2\pi q_{\mathsf{D}}\lambda_{\mathrm{f}} r \exp(-\pi r^2 q_{\mathsf{D}}\lambda_{\mathrm{f}})dr \\
&= \frac{q_{\mathsf{D}}\lambda_{\mathrm{f}}(1-\exp(\pi \mathrm{R}_{\mathsf{HO}}^2(q_{\mathsf{D}}\lambda_{\mathrm{f}}(1+\rho(\gamma_{\mathrm{f}},\alpha)) + (\lambda_{\mathrm{m}}P_{\mathrm{m}}^{2/\alpha} + (1-q_{\mathsf{D}})\lambda_{\mathrm{f}}Q_{\mathrm{f}}^{2/\alpha})(\gamma_{\mathrm{f}}/P_{\mathrm{f}})^{2/\alpha}C(\alpha))))}{q_{\mathsf{D}}\lambda_{\mathrm{f}}(1+\rho(\gamma_{\mathrm{f}},\alpha)) + (\lambda_{\mathrm{m}}P_{\mathrm{m}}^{2/\alpha} + (1-q_{\mathsf{D}})\lambda_{\mathrm{f}}Q_{\mathrm{f}}^{2/\alpha})(\gamma_{\mathrm{f}}/P_{\mathrm{f}})^{2/\alpha}C(\alpha)} \qquad (43)
\end{aligned}$$

interfering FAPs in downlink (conditioned on being at least r away), the MBSs, and the FAPs in downlink, respectively, and the pdf of the location of the nearest downlink FAP. Now let s be the distance to the nearest MBS. We compute the success probability conditioned on the event that the user connects to the macro tier:

$$\begin{aligned}
&\mathbb{P}(\mathsf{D}|r > \mathrm{R}_{\mathsf{HO}}) \\
&\overset{(c)}{=} \int_{s=0}^{\infty} \mathbb{P}(\mathsf{D}|s, r > \mathrm{R}_{\mathsf{HO}}) f_{\mathrm{m}}(s)ds \\
&\overset{(d)}{=} \int_{s=0}^{\infty} \exp(-\pi s^2 \lambda_{\mathrm{m}}\rho(\gamma_{\mathrm{m}},\alpha)) \\
&\exp(-\pi s^2 q\lambda_{\mathrm{f}}(\gamma_{\mathrm{m}}P_{\mathrm{f}}/P_{\mathrm{m}})^{2/\alpha}\int_{S_0}^{\infty} 1/(1+z^{\alpha/2})dz) \\
&\exp(-\pi s^2(1-q_{\mathsf{D}})\lambda_{\mathrm{f}}(Q_{\mathrm{f}}\gamma_{\mathrm{m}}/P_{\mathrm{m}})^{2/\alpha}C(\alpha)) f_{\mathrm{m}}(s)ds \qquad (44)
\end{aligned}$$

where $S_0 = (\mathrm{R}_{\mathsf{HO}}^2/s^2)(P_{\mathrm{m}}/P_{\mathrm{f}}\gamma_{\mathrm{m}})^{2/\alpha}$ and $f_{\mathrm{m}}(s) = 2\pi\lambda_{\mathrm{m}} s\exp(-\pi\lambda_{\mathrm{m}}s^2)$ the pdf of s. Here, in (c) we condition on the event that the nearest MBS is at s, and (d) splits up the success probability of a single transmission into the Laplace transforms of the interference due to following: the MBS (conditioned on being at least s away), the uplink FAPs, and the downlink FAPs, and the pdf of the location of the nearest MBS. The derivation of the Laplace transform of the interference due to downlink FAPs conditioned on that it is located at least R_{HO} follows from letting $s = \mathrm{R}_{\mathsf{HO}}$ in (39).

F. Proof of Theorem 4

We first begin by deriving (19) as follows:

$$\begin{aligned}
&\mathbb{P}_{\mathrm{m}}(\mathsf{U}, t) \\
&= \int_0^{\infty} \mathbb{E}_{\tilde{\Theta},\Phi,\tilde{\Phi}}\Bigg[\exp\Bigg(-\frac{\eta_{\mathrm{m}} r^{\alpha}}{Q_{\mathrm{m}}}\Bigg(\sum_{x\in\tilde{\Theta}\setminus\{0\}} Q_{\mathrm{m}} h_x x^{-\alpha} \\
&+ \sum_{y\in\Phi} P_{\mathrm{f}} h_y y^{-\alpha} + \sum_{z\in\tilde{\Phi}} Q_{\mathrm{f}} h_z z^{-\alpha}\Bigg)\Bigg)\Bigg] f(r)\mathrm{d}r \\
&\overset{(a)}{=} \int_0^{\infty} \mathbb{E}_{\tilde{\Theta}}\Bigg[\exp\Bigg(-\eta_{\mathrm{m}} r^{\alpha}\Big(\sum_{x\in\tilde{\Theta}\setminus\{0\}} (Q_{\mathrm{m}}/Q_{\mathrm{m}}) h_x x^{-\alpha}\Big)\Bigg)\Bigg] \\
&\mathbb{E}_{\Phi^{\mathsf{D}}}\Bigg[\exp\Bigg(-\eta_{\mathrm{m}} r^{\alpha}\Big(\sum_{y\in\Phi^{\mathsf{D}}} (P_{\mathrm{f}}/Q_{\mathrm{m}}) h_y y^{-\alpha}\Big)\Bigg)\Bigg] \\
&\mathbb{E}_{\Phi^{\mathsf{U}}}\Bigg[\exp\Bigg(-\eta_{\mathrm{m}} r^{\alpha}\Big(\sum_{z\in\Phi^{\mathsf{U}}} (Q_{\mathrm{f}}/Q_{\mathrm{m}}) h_z z^{-\alpha}\Big)\Bigg)\Bigg] f(r)\mathrm{d}r \\
&\overset{(b)}{=} \int_0^{\infty} \exp\Bigg(-\pi r^2\big(\mu_{\mathrm{m}} Q_{\mathrm{m}}^{\frac{2}{\alpha}} + q\lambda_{\mathrm{f}} P_{\mathrm{f}}^{\frac{2}{\alpha}} \\
&\qquad + (1-q)\lambda_{\mathrm{f}} Q_{\mathrm{f}}^{\frac{2}{\alpha}}\big) C(\alpha)(\eta_{\mathrm{m}}/Q_{\mathrm{m}})^{\frac{2}{\alpha}}\Bigg) f(r)\mathrm{d}r \\
&\overset{(c)}{=} \frac{\lambda_{\mathrm{m}}}{\lambda_{\mathrm{m}} + \big(\mu_{\mathrm{m}} + q\lambda_{\mathrm{f}}\big(\frac{P_{\mathrm{f}}}{Q_{\mathrm{m}}}\big)^{\frac{2}{\alpha}} + (1-q)\lambda_{\mathrm{f}}\big(\frac{Q_{\mathrm{f}}}{Q_{\mathrm{m}}}\big)^{\frac{2}{\alpha}}\big) C(\alpha)\eta_{\mathrm{m}}^{\frac{2}{\alpha}}}
\end{aligned}$$

where (a) by the independence of the PPPs; (b) using Slivnyak's Theorem and the Laplace transforms of the macro and femto tier interference terms; and (c) integrating with respect to $f(r)$, the pdf of the location of the nearest MBS,

to obtain the desired result. Next, we derive (20) as follows:

$$
\begin{aligned}
&\mathbb{P}_{\mathrm{f,U}}(\leftrightarrow,t)\\
&= q\mathbb{E}_{\tilde{\Theta},\Phi,\tilde{\Phi}}\Bigg[\exp\Bigg(-\frac{\gamma_{\mathrm{f}}r^{\alpha}}{P_{\mathrm{f}}}\Bigg(\sum_{x\in\tilde{\Theta}}Q_{\mathrm{m}}h_x x^{-\alpha}\\
&\qquad+\sum_{y\in\Phi\setminus 0}P_{\mathrm{f}}h_y y^{-\alpha}+\sum_{z\in\tilde{\Phi}\setminus 0}Q_{\mathrm{f}}h_z z^{-\alpha}\Bigg)\Bigg)\Bigg]\\
&\quad+(1-q)\mathbb{E}_{\tilde{\Theta},\Phi,\tilde{\Phi}}\Bigg[\exp\Bigg(-\frac{\gamma_{\mathrm{f}}r^{\alpha}}{Q_{\mathrm{f}}}\Bigg(\sum_{x\in\tilde{\Theta}}Q_{\mathrm{m}}h_x x^{-\alpha}\\
&\qquad+\sum_{y\in\Phi\setminus 0}P_{\mathrm{f}}h_y y^{-\alpha}+\sum_{z\in\tilde{\Phi}\setminus 0}Q_{\mathrm{f}}h_z z^{-\alpha}\Bigg)\Bigg)\Bigg]\\
&\overset{(a)}{=} q\mathbb{E}_{\tilde{\Theta}}\Bigg[\exp\Bigg(-\gamma_{\mathrm{f}}r^{\alpha}\Big(\sum_{x\in\tilde{\Theta}}(Q_{\mathrm{m}}/P_{\mathrm{f}})h_x x^{-\alpha}\Big)\Bigg)\Bigg]\\
&\quad\mathbb{E}_{\Phi^{\mathrm{D}}}\Bigg[\exp\Bigg(-\gamma_{\mathrm{f}}r^{\alpha}\Big(\sum_{y\in\Phi^{\mathrm{D}}}(P_{\mathrm{f}}/P_{\mathrm{f}})h_y y^{-\alpha}\Big)\Bigg)\Bigg]\\
&\quad\mathbb{E}_{\Phi^{\mathrm{U}}}\Bigg[\exp\Bigg(-\gamma_{\mathrm{f}}r^{\alpha}\Big(\sum_{z\in\Phi^{\mathrm{U}}}(Q_{\mathrm{f}}/P_{\mathrm{f}})h_z z^{-\alpha}\Big)\Bigg)\Bigg]\\
&\quad+(1-q)\mathbb{E}_{\tilde{\Theta}}\Bigg[\exp\Bigg(-\gamma_{\mathrm{f}}r^{\alpha}\Big(\sum_{x\in\tilde{\Theta}}(Q_{\mathrm{m}}/Q_{\mathrm{f}})h_x x^{-\alpha}\Big)\Bigg)\Bigg]\\
&\quad\mathbb{E}_{\Phi^{\mathrm{D}}}\Bigg[\exp\Bigg(-\gamma_{\mathrm{f}}r^{\alpha}\Big(\sum_{y\in\Phi^{\mathrm{D}}}(P_{\mathrm{f}}/Q_{\mathrm{f}})h_y y^{-\alpha}\Big)\Bigg)\Bigg]\\
&\quad\mathbb{E}_{\Phi^{\mathrm{U}}}\Bigg[\exp\Bigg(-\gamma_{\mathrm{f}}r^{\alpha}\Big(\sum_{z\in\Phi^{\mathrm{U}}}(Q_{\mathrm{f}}/Q_{\mathrm{f}})h_z z^{-\alpha}\Big)\Bigg)\Bigg]\\
&\overset{(b)}{=} q\exp\Bigg(-\pi\frac{R_{\mathrm{f}}^2}{P_{\mathrm{f}}^{\frac{2}{\alpha}}}\big(\lambda_{\mathrm{m}}Q_{\mathrm{m}}^{\frac{2}{\alpha}}+q\lambda_{\mathrm{f}}P_{\mathrm{f}}^{\frac{2}{\alpha}}\\
&\qquad+(1-q)\lambda_{\mathrm{f}}Q_{\mathrm{f}}^{\frac{2}{\alpha}}\big)C(\alpha)\gamma_{\mathrm{f}}^{\frac{2}{\alpha}}\Bigg)\\
&\quad+(1-q)\exp\Bigg(-\pi\frac{R_{\mathrm{f}}^2}{Q_{\mathrm{f}}^{\frac{2}{\alpha}}}\big(\mu_{\mathrm{m}}Q_{\mathrm{m}}^{\frac{2}{\alpha}}+q\lambda_{\mathrm{f}}P_{\mathrm{f}}^{\frac{2}{\alpha}}\\
&\qquad+(1-q)\lambda_{\mathrm{f}}Q_{\mathrm{f}}^{\frac{2}{\alpha}}\big)C(\alpha)\eta_{\mathrm{f}}^{\frac{2}{\alpha}}\Bigg)
\end{aligned}
$$

where (a) by the independence of the PPPs and the Slivnyak's Theorem; and (b) by the Laplace transforms of the macro and femto tier interference terms.

REFERENCES

[1] H. Claussen, L. T. W. Ho, and L. G. Samuel, "An overview of the femtocell concept," *Bell Labs Tech. Journal*, vol. 13, no. 1, pp. 221–246, 2008.

[2] V. Chandrasekhar, J. G. Andrews, and A. Gatherer, "Femtocell networks: A survey," *IEEE Commun. Mag.*, vol. 46, no. 9, pp. 59–67, Sep. 2008.

[3] J. Hoydis, M. Kobayashi, and M. Debbah, "Green small-cell networks," *IEEE Veh. Technol. Mag.*, vol. 6, no. 1, pp. 37–43, Mar. 2011.

[4] D. López-Pérez, İ. Güvenc, G. de la Roche, M. Kountouris, T. Q. S. Quek, and J. Zhang, "Enhanced intercell interference coordination challenges in heterogeneous networks," *IEEE Wireless Commun. Mag.*, vol. 18, no. 3, pp. 22–30, Jun. 2011.

[5] K. Zheng, Y. Wang, W. Wang, M. Dohler, and J. Wang, "Energy-efficient wireless in-home: The need for interference-controlled femtocells," *IEEE Wireless Commun. Mag.*, vol. 18, no. 6, pp. 36–44, Dec. 2011.

[6] Y. Jeong, H. Shin, and M. Z. Win, "Superanalysis of optimum combining with application to femtocell networks," *IEEE J. Sel. Areas Commun.*, vol. 30, no. 4, Apr. 2012.

[7] M. Haenggi and R. K. Ganti, "Interference in large wireless networks," *Found. Trends Netw.*, vol. 3, no. 2, 2009.

[8] M. Z. Win, P. C. Pinto, and L. A. Shepp, "A mathematical theory of network interference and its applications," *Proc. of the IEEE*, vol. 97, no. 2, pp. 205–230, Feb. 2009.

[9] M. Haenggi, J. G. Andrews, F. Baccelli, O. Dousse, and M. Franceschetti, "Stochastic Geometry and Random Graphs for the Analysis and Design of Wireless Networks," *IEEE J. Sel. Areas Commun.*, vol. 27, no. 7, pp. 1029–1046, Sep. 2009.

[10] A. Rabbachin, T. Q. S. Quek, H. Shin, and M. Z. Win, "Cognitive network interference," *IEEE J. Sel. Areas Commun.*, vol. 29, no. 2, pp. 480–493, Feb. 2011.

[11] J. G. Andrews, F. Baccelli, and R. K. Ganti, "A tractable approach to coverage and rate in cellular networks," *IEEE Trans. Commun.*, vol. 59, no. 11, pp. 3122–3134, Nov. 2011.

[12] V. Chandrasekhar and J. G. Andrews, "Spectrum allocation in tiered cellular networks," *IEEE Trans. Commun.*, vol. 57, no. 10, pp. 3059–3068, Oct. 2009.

[13] ——, "Uplink capacity and interference avoidance for two-tier femtocell networks," *IEEE Trans. Wireless Commun.*, vol. 8, no. 7, pp. 3498–3509, Jul. 2009.

[14] W. C. Cheung, T. Q. S. Quek, and M. Kountouris, "Throughput optimization, spectrum sharing, and femtocell access in two-tier femtocell networks," *IEEE J. Sel. Areas Commun.*, vol. 30, no. 4, pp. 561–574, Apr. 2012.

[15] M. Andrews, V. Capdevielle, A. Feki, and P. Gupta, "Autonomous spectrum sharing for unstructured cellular networks with femtocells," *Bell Labs Tech. Journal*, vol. 15, no. 3, pp. 85–97, Dec. 2010.

[16] S. Haykin, "Cognitive radio: Brain-empowered wireless communications," *IEEE J. Sel. Areas Commun.*, vol. 23, no. 2, pp. 210–220, Feb. 2005.

[17] A. Goldsmith, S. A. Jafar, I. Marić, and S. Srinivasa, "Breaking spectrum gridlock with cognitive radios: An information theoretic perspective," *Proc. IEEE*, vol. 97, no. 5, pp. 894–914, May 2009.

[18] Y.-C. Liang, K.-C. Chen, G. Y. Li, and P. Mähönen, "Cognitive radio networking and communications: An overview," *IEEE Trans. Veh. Technol.*, vol. 60, no. 7, pp. 3386–3407, Sep. 2011.

[19] G. P. Villardi, Y. D. Alemseged, C. Sun, C.-S. Sum, T. H. Nguyen, T. Baykas, and H. Harada, "Enabling coexistence of multiple cognitive networks in TV white space," *IEEE Wireless Commun. Mag.*, vol. 18, no. 4, pp. 32–40, Aug. 2011.

[20] A. Adhikary, V. Ntranos, and G. Caire, "Cognitive femtocells: Breaking the spatial reuse barrier of cellular systems," in *Proc., Information Theory and its Applications (ITA)*, San Diego, CA, Feb. 2011.

[21] S.-M. Cheng, S.-Y. Lien, F.-S. Chu, and K.-C. Chen, "On exploiting cognitive radio to mitigate interference in macro/femto heterogeneous networks," *IEEE Wireless Commun. Mag.*, vol. 18, no. 3, pp. 40–47, Jun. 2011.

[22] S.-Y. Lien, Y.-Y. Lin, and K.-C. Chen, "Cognitive and game-theoretical radio resource management for autonomous femtocells with QoS guarantees," *IEEE Trans. Wireless Commun.*, vol. 10, no. 7, pp. 2196–2206, Jul. 2011.

[23] S. Yun, S. Y. Park, Y. Lee, D. Park, Y. Kim, K. Kim, and C. G. Kang, "Hybrid division duplex system for next-generation cellular services," *IEEE Trans. Veh. Technol.*, vol. 56, no. 5, pp. 3040–3059, Sep. 2007.

[24] C. H. M. de Lima, M. Bennis, K. Ghaboosi, and M. Latva-aho, "Interference management for self-organized femtocells towards green networks," in *Proc., IEEE PIMRC*, Istanbul, Turkey, Sep. 2010, pp. 352–356.

[25] F. Baccelli, B. Blaszczyszyn, and P. Mühlethaler, "Stochastic analysis of spatial and opportunistic ALOHA," *IEEE J. Sel. Areas Commun.*, vol. 27, no. 7, pp. 1105–1119, Sep. 2009.